



# Evaluation of hydrogeochemical processes and saltwater intrusion in the coastal aquifers in the southern part of Puri District, Odisha, India

Jyoti Kushawaha<sup>1</sup> · Janardhana Raju Nandimandalam<sup>1</sup> · Sughosh Madhav<sup>2</sup> · Amit Kumar Singh<sup>1,3</sup>

Received: 7 March 2023 / Accepted: 4 March 2024 / Published online: 14 March 2024  
© The Author(s), under exclusive licence to Springer-Verlag GmbH Germany, part of Springer Nature 2024

## Abstract

Groundwater is widely regarded as being among the freshwater natural resources with the lowest levels of contamination. Nevertheless, the saltwater intrusion has resulted in the contamination of groundwater in coastal regions with lower elevation. The rationale of the present work is to investigate the chemistry of groundwater, to identify the various facies of groundwater, to identify the processes that influence groundwater chemistry and saltwater intrusion, and to evaluate the groundwater's aptness for use in drinking and farming. In order to gain an understanding of the groundwater quality as well as the salinization process that occurs in coastal aquifers as a result of hydrogeochemical processes, a total of 108 groundwater samples (54 each in pre- and post-monsoon) were taken and analyzed for several physiochemical parameters in the southern part of the Puri district in the Indian state of Odisha. The data has undergone analysis and examination to identify the factors (such as hydrological facies, potential solute source in water, and salinization process) that contribute to groundwater salinity. The result showed the chemistry controlling processes of rock-water interaction as per Gibbs diagram. The majority of shallow aquifers exhibit the Na-Cl type of facies as per the Piper plot. A total of 37% pre-monsoon and 33% post-monsoon samples having  $\text{Na}^+/\text{Cl}^-$  ratio below the threshold of 0.86 indicating the influence of saltwater intrusion. In both seasons, it was observed that 74% of the samples exhibited a  $\text{Na}^+$  concentration that exceeded the permissible limit set by the World Health Organization (WHO) for drinking purposes. The findings indicate that most groundwater failed to pass safe drinking water and irrigation standards due to saltwater intrusion. Consequently, the monitoring of coastal aquifer quality has become imperative in order to ensure the sustainability of aquifers and the development of groundwater resources. This is because coastal aquifers are highly vulnerable to saltwater intrusion, primarily as a result of the extensive extraction of groundwater for diverse purposes.

**Keywords** Coastal aquifer · Hydrogeochemical processes · Saltwater intrusion · Ionic ratio · SWMI · Groundwater quality

## Introduction

While the Earth possesses an ample supply of water, the availability of potable freshwater is relatively limited. Thus, the lion's share of water system employment is saline. This saltwater intrusion (SWI) is due to density and pressure differences in coastal aquifers, a common phenomenon. However, it has increased in recent years due to enhanced anthropogenic activities and industrialization (De Pippo et al. 2006; Huang et al. 2013; Kumar et al. 2023). Saline water ingress deteriorated the groundwater quality, especially around the coasts.

SWI is widespread in numerous coastal regions worldwide. It is one of the main reasons of destruction of the

---

Responsible Editor: V.V.S.S. Sarma

---

✉ Janardhana Raju Nandimandalam  
rajunj7@gmail.com

<sup>1</sup> School of Environmental Sciences, Jawaharlal Nehru University, New Delhi 110067, India

<sup>2</sup> Department of Civil Engineering, Jamia Milia Islamia, New Delhi 110025, India

<sup>3</sup> Department of Environmental Studies, Deshbandhu College, University of Delhi, New Delhi 110019, India

fresh coastal aquifers (Bear et al. 1999; Purnama and Marfai 2012). Groundwater quality mainly depends on the concentration of the dissolved ions (Raju et al. 2009; 2011 and 2014; Patel et al. 2016; Madhav et al. 2018 and 2021). The tremendous water demand has significantly intensified groundwater extraction, mainly in densely populated coastal areas (Famiglietti 2014). Excessive groundwater extraction compared to natural recharge causes lowering of the water table in coastal aquifers, resulting SWI (Sahagian 2000; Chidambaram et al. 2018; Selvakumar and Chandrasekar 2021). The intensification of groundwater salinity is due to the inflow saline water naturally as well anthropogenic causes. These coastal aquifers decaying is caused by various natural processes including the infringement of sea water, highly pressurized brines stabbing into fresh groundwater, and by underground dissolution of soluble salts inventing in neighboring country rocks and also by water–rock interaction (Vengosh and Rosenthal 1994; Glynn and Plummer 2005; Cloutier et al. 2008; Idowu and Lasisi 2020; Etikala et al. 2021). Moreover, increasing trend of temperature due to global warming leads to sea level rise and overexploitation of fresh water in overpopulated coastal region have led to SWI (Oude Essink 2001; Ferguson and Gleeson 2012). Groundwater quality declines due to SWI into coastal confined or unconfined aquifers due to a difference in fluid density (Nair et al. 2015). Identification of ‘saltwater–freshwater’ mixing in the coastal aquifer has been identified by various researchers using different ionic ratios like  $\text{Na}^+/\text{Cl}^-$  ratio (Vengosh and Rosenthal 1994),  $\text{Ca}^{2+}/\text{Mg}^{2+}$  ratio (Moujabber et al. 2006),  $\text{Cl}^-/\text{Br}^-$  ratio (Nair et al. 2015), and  $\text{Cl}^-/\text{HCO}_3^-$  ratio (Chidambaram et al. 2018). The saltwater mixing index is an identification of SWI in the freshwater aquifer (Mondal et al. 2011; Idowu et al. 2017). The current study examined and discussed the saline water intrusion processes in the region of Puri district.

Saltwater mixing remains the major degrading factor in the coastal aquifer of the Puri district. As a result, over 50% of fresh groundwater in the south Mahanadi delta including Puri, Konark, and Rabanagaon regions have become either brackish or saline (Radhakrishna 2001). A study carried out by Mohanty and Rao (2019) in Puri district, revealed that the TDS value increases from inland recharge region to the shoreline discharge region based on the groundwater flow path and the facies changes from  $\text{Na–K–HCO}_3$  to  $\text{Na–Mg–Cl}$  type. Mohapatra et al. (2011) and Vijay et al. (2011) studied the groundwater of Puri city; it was revealed that septic tank and soak pits are the cause of groundwater pollution along with the hydrological process of SWI in summers.

The similar research work was carried out earlier (Mohapatra et al. 2011; Prusty et al. 2018 and Vijay et al. 2011) but the studies on groundwater quality is a dynamic phenomenon. The earlier work covers some different parts of the Puri regions from the current work. The present

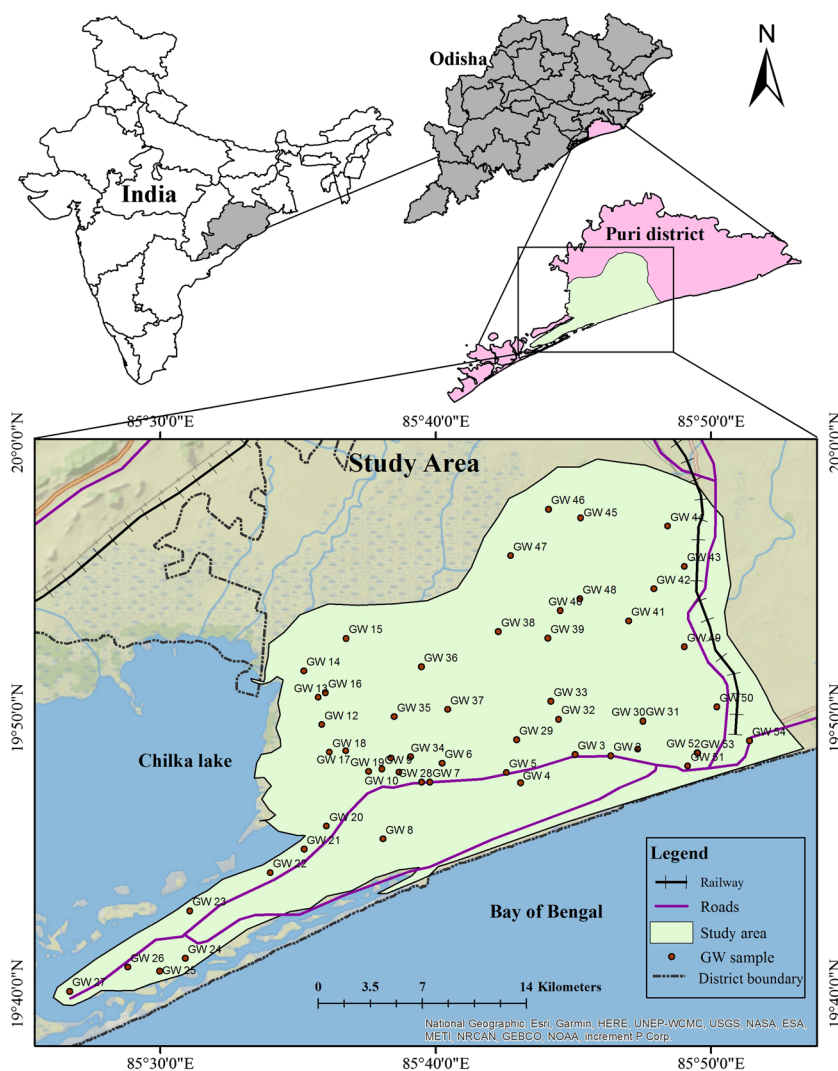
work covers more wide area and provide recent data about the groundwater quality and saltwater mixing. The earlier studies were more focused on groundwater quality where the current study includes the saltwater mixing also. This study is being carried out to understand the groundwater pollution due to anthropogenic activities and SWI and the acceptability of water for diverse applications in the sectors of agricultural and domestic functions. In the current study, hydrogeochemical assessment of groundwater samples in the coastal region of Puri was carried out and the saltwater mixing was also examined in the freshwater aquifers.

## Study area and geology

The study region chosen is between longitude  $85^\circ 25' 30''$  E to  $85^\circ 52' 30''$  E and  $19^\circ 40' 0''$  N to  $19^\circ 58' 30''$  N with a geomorphological area of  $670 \text{ km}^2$ . Mainly, the Mahanadi delta covered this area (Fig. 1). The tributaries drain of the Mahanadi River in the Puri region, which supplies a maximum of the fresh surface water before it empties into the Bay of Bengal. However, the population explosion, overexploitation, intense urbanization, industrialization, and excessive use of fertilizers gave birth to a water crisis (Mohapatra et al. 2011; Vijay et al. 2011). The climate of the Puri district may be described as tropical, and the district receives an average of 1449 mm of rainfall during the monsoon season. The annual groundwater recharge in the study area is estimated by 55.1 to 348 mm/yr (Sahoo 2014). The southwest monsoon is the primary mechanism responsible for precipitation in the district. Flood is typical in this area due to high rainfall, frequent cyclones and storm surges (CGWB 2017). Physiographically, there are two natural divisions: the first is a saline marshy zone beside the coast, and the second is a tenderly sloping plain (alluvium with some patches of laterite). Geomorphology is broadly characterized by fluvial, coastal, lacustrine, and water bodies. The older and active floodplains indicate fluvial origin. Dune elevation ranges 15–27 m close to the coastline, while height remains less than 27 m above sea level, with a significant part representing the elevation range of 5–10 m (Sahu et al. 2018).

The quaternary formations are common in the study area, while Tertiary and Archean are over-lying by alluvium, coastal marshy plains, and laterite in patches. The older alluvium is exposed in the northwestern parts containing a sequence of sand, clay, and kankars of gray to brown. The younger alluvium occupies the remaining area, which consists of an admixture of silt, sand, gravel, and pebble to a changeable extent. These layers rise in width towards the sea (Radhakrishna 2001). The water table varies from 1 to 10 m below ground level (bgl) and its level shifts according to the rainfall pattern (Mohanty and Rao 2019). The ordinary groundwater extraction formations are dug wells and shallow and deep tube wells (CGWB 2017).

**Fig. 1** Physiography and groundwater sample location in the study area



## Material and methods

A total of 108 groundwater samples were taken from shallow aquifers of the study area, with 54 taken before the monsoon season began in May 2017 and 54 taken after monsoon season in November 2017. Standard procedures of the American Public Health Association were used for collecting, preserving, and succeeding examination of the groundwater samples (APHA 2012). The samples for major ions were collected in ½-L sample bottles (Tarsons polyethylene), pre-treated in a solution of nitric acid diluted 1:1 over 24 h. Sampling bottles were washed with deionized water to avoid any redundant contamination. The samples were cleaned of suspended sediments before the chemical test. In order to remove the suspended sediments, each sample was run through vacuum filtration equipment and filtered using filter paper with a pore size of 0.45-µm Millipore.

Physical constituents pH and electrical conductivity (EC) were calculated in the field with portable electrodes (pH/Cond

340i SET 1 Electrode). The measurement of  $\text{Ca}^{2+}$ ,  $\text{HCO}_3^-$ ,  $\text{Cl}^-$ , and hardness was carried out by titration method.  $\text{Mg}^{2+}$  and alkalinity were calculated by the calculation method, while  $\text{F}^-$  and  $\text{Br}^-$  were measured by the ISE method (ion selective electrode, Thermo-scientific Orion 4-star).  $\text{Na}^+$  and  $\text{K}^+$  were analyzed by a flame photometer (ELICO model CL-378).  $\text{SO}_4^{2-}$ ,  $\text{NO}_3^-$ , and  $\text{SiO}_2$  were quantified by a UV–visible double beam spectrophotometer. The precision of the investigation was confirmed by calculating ionic equilibrium. The electro-neutrality (EN %) of the data within the  $\pm 5$ . The map preparation was done in a GIS environment. Microsoft Excel and (Statistical Package for Social Sciences) SPSS 21 were used for various statistical calculations, Gibbs diagram, and saturation indices. PHREEQC Interactive 2.12 and Aquachem 4.0 have been used for geochemical modelling to generate the saturation indices value. The SI, or saturation index, is a mathematical representation of the relationship between the ion activity product (IAP) and the mineral equilibrium constant (Ksp) at a

specific temperature. This definition was established by Freeze and Cherry in 1979. Saltwater mixing index (SWMI) were calculated using major ions in seawater including Na<sup>+</sup>, Mg<sup>2+</sup>, Cl<sup>-</sup>, and SO<sub>4</sub><sup>2-</sup>. The threshold value were estimated by the inflection point scaled on cumulative probability curve (Kumar et al. 2016).

## Result and discussion

### General geochemistry

The pH value ranges from 5.76 to 7.64 with a mean value of 6.91 in the pre-monsoon and from 6.34 to 8.14 with a mean value of 7.31 in the post-monsoon, respectively. The results shows that the pH of the study area is slightly alkaline in post-monsoon which could be due to the influx of bicarbonate ions in groundwater aquifer system through rainwater percolation (Masood et al. 2022). All the values of pH in both the seasons is under the permissible

limit recommended by WHO (2006) and BIS (2012). The concentration of EC in the groundwater ranges from 223 to 7600 mg/L with a mean value of 2677.93 mg/L in the pre-monsoon and from 125 to 5500 mg/L with a mean value of 2389.57 mg/L in post-monsoon, correspondingly (Table 1). High values of EC are observed in the pre-monsoon as compared to post-monsoon, which could be due to the evaporation dominance character and halite enrichment in the groundwater in the pre-monsoon. Approximately 54% samples fall under very high salinity hazard (> 2250 μS/cm). The concentration of TDS in the groundwater ranges from 149 to 3513 mg/L with a mean of 1552 mg/L in the pre-monsoon season and from 125.96 to 3377 mg/L with a mean of 1532 mg/L in the post-monsoon season (Table 1).

Among the cationic constituents, the dominant cation was Na<sup>+</sup> with a range of 33.4 to 950.6 mg/L with a mean of 397.35 mg/L in pre-monsoon and 35.7 to 890.4 mg/L with a mean of 414.01 mg/L in post-monsoon followed by Ca<sup>2+</sup>, Mg<sup>2+</sup>, and K<sup>+</sup>. The details are given for cationic

**Table 1** Statistical summary of different physiochemical parameters in groundwater samples

Parameters	Pre-monsoon				Post-monsoon			
	Min	Max	Mean	St dev	Min	Max	Mean	St dev
Ca <sup>2+</sup>	12	288	59.26	45.26	8	172	54.2	40.33
Mg <sup>2+</sup>	2.2	183.34	43.33	37.47	0.98	243.51	36.15	37.05
Na <sup>+</sup>	33.4	950.6	397.35	258.24	35.7	890.4	414.01	243.66
K <sup>+</sup>	0.5	39.4	3.91	5.72	0.3	23.9	2.89	3.59
HCO <sub>3</sub> <sup>-</sup>	40	832	306.17	155.04	32	612	275.39	117.42
Cl <sup>-</sup>	28	1650	611.17	479.97	46	1510	613.2	406.38
F <sup>-</sup>	0.02	1.7	0.38	0.39	0	2.7	0.64	0.58
Br <sup>-</sup>	0.54	33	8.95	7.1	0.5	22	8.39	5.94
SO <sub>4</sub> <sup>2-</sup>	1.23	182	55.37	37.11	2.47	126.6	64.22	32.3
NO <sub>3</sub> <sup>-</sup>	0	423	30.49	81.13	3.75	231	26.9	46.29
SiO <sub>2</sub>	15.01	35.26	29.38	5.03	0.51	53.14	41.64	8.49
Hardness	60	1284	325.99	245.57	24	1052	284.09	210.82
pH	5.76	7.64	6.91	0.35	6.34	8.04	7.31	0.42
EC	223	7600	2677.93	1798.19	188	5500	2389.57	1437.19
TDS	149	3513	1552.36	921.11	125.96	3377	1532.63	897.61
Ionic ratio and indices								
Na <sup>+</sup> /Cl <sup>-</sup>	0.61	3.58	1.19	0.49	0.64	3.94	1.16	0.46
Ca <sup>2+</sup> /Mg <sup>2+</sup>	0.21	6.06	1.21	0.99	0.05	14.71	1.62	2.46
K <sup>+</sup> /Cl <sup>-</sup>	0.001	0.058	0.01	0.013	0.001	0.063	0.007	0.011
Br <sup>-</sup> /Cl <sup>-</sup>	0.002	0.026	0.015	0.005	0.002	0.03	0.014	0.005
Cl <sup>-</sup> /HCO <sub>3</sub> <sup>-</sup>	0.053	2.7	0.58	0.63	0.09	2.73	0.44	0.46
SWMI	0.291	11.62	4.762	3.180	0.53	15.66	6.679	4.2
SW (%)	-0.074	8.5	3.155	2.49	0.021	7.76	3.018	2.15
CIA I	-2.59	0.39	-0.20	0.49	-2.95	0.36	-0.16	0.46
CIA II	-0.98	2.74	0.05	0.72	-0.94	1.31	-0.12	0.49
r1	-86.10	29.08	-0.36	13.56	-4.18	10.18	-1.19	3.14
r2	-84.91	29.24	-0.20	13.45	-4.17	10.22	1.26	3.14

Concentrations are in mg/L, except pH and EC (μS/cm)



constituents in the Table 1. Among major anionic concentrations,  $\text{Cl}^-$  was the dominant ion having a range of 28 to 1650 mg/L with a mean of 611.17 mg/L in pre-monsoon and 46 to 1510 mg/L with a mean 613.2 mg/L in post-monsoon followed by  $\text{HCO}_3^-$ ,  $\text{SO}_4^{2-}$ , and  $\text{NO}_3^-$  (Table 1). Moreover,  $\text{Br}^-$  ranged from 0.54 to 33 mg/L with a mean value of 8.95 mg/L in pre-monsoon and 0.5 to 22 mg/L with mean value of 8.39 mg/L in post-monsoon (Table 1). For the cations chemistry, 72% and 85% samples show  $\text{Na}^+ > \text{Ca}^{2+} > \text{Mg}^{2+} > \text{K}^+$  type of water and the remaining 28% and 19% samples show  $\text{Na}^+ > \text{Mg}^{2+} > \text{Ca}^{2+} > \text{K}^+$  type of water in pre- and post-monsoon, correspondingly. Further, the anion chemistry indicates 63% and 81% of samples show  $\text{Cl}^- > \text{HCO}_3^- > \text{SO}_4^{2-} > \text{NO}_3^-$  type of water and the remaining 37% and 19% of samples show  $\text{HCO}_3^- > \text{Cl}^- > \text{SO}_4^{2-} > \text{NO}_3^-$  type of water in pre- and post-monsoon, correspondingly.

### Hydrogeochemical facies and water type

Groundwater occurrence modes within an aquifer that vary in chemical composition are referred to as “hydrogeochemical facies” (Patel et al. 2016). The lithology, solution kinetics, and aquifer flow patterns influence the water facies. When considered alongside distribution maps and hydrochemical sections, hydrochemical diagrams help to analyze evolutionary tendencies, particularly in groundwater systems (Raju et al. 2011).

#### Piper’s diagram

The Piper diagram (Piper 1944) was used to classify the hydrochemical facies of water according to their ionic dominance.  $\text{Na}^+$  and  $\text{Cl}^-$  are predominant among all ions in the groundwater samples. For cationic facies, it is noted that 85% and 91% of samples fall under  $\text{Na}^+ + \text{K}^+$  type, whereas 15% and 9% of samples fall under no dominance type in pre- and post-monsoon, correspondingly. For anionic facies, it was noted that 85% and 91% of samples fall under  $\text{Cl}^-$  type, 11% and 4% of samples fall under  $\text{HCO}_3^-$  type of water, and 4% and 5% of samples fall under no dominance type in pre- and post-monsoon, correspondingly (Fig. 2).

The results of the Piper diagram showed that the Na-Cl type of facies was present in 81% of pre-monsoon samples and 89% of post-monsoon samples, correspondingly. In the diamond plot, the Na-Cl composition of the water served as an indicator of the salinization process. Rest of the samples lie in Na- $\text{HCO}_3$ -Cl and Na- $\text{HCO}_3$  type of water.

#### Gibbs diagram

Gibb’s value for cations (Gibb’s I) is a plot between TDS (mg/L) and  $(\text{Na}^+ + \text{K}^+)/(\text{Na}^+ + \text{K}^+ + \text{Ca}^{2+})$  (meq/L). Gibb’s I ranged from 0.531 to 0.968 with a mean value

of 0.829 in pre-monsoon and from 0.571 to 0.978 with a mean value of 0.841 in post-monsoon. Moreover, Gibb’s value for anions (Gibb’s II) is a plot between TDS (mg/L) and  $\text{Cl}^-/(\text{Cl}^- + \text{HCO}_3^-)$  (meq/L). Gibb’s II ranged from 0.271 to 0.949 with a mean value of 0.701 in pre-monsoon and from 0.268 to 0.915 with a mean value of 0.733 in post-monsoon. According to Gibb’s I, approximately 67% and 61% of the samples show evaporation dominance and 33% and 39% of the samples show rock dominance as the principal controlling processes for groundwater chemistry in pre- and post-monsoon, correspondingly (Fig. 3a). In Gibb’s II, approximately, 67% and 63% of the samples show evaporation dominance and 33% and 37% of the samples show rock dominance in pre- and post-monsoon, correspondingly. The Gibbs diagram suggest that evaporation dominance followed by rock dominance are the primary chemistry controlling process for cationic and anionic composition of water (Fig. 3b) (Suguna and Sherene 2019). An increased level of evaporation or human activities contributes to higher total dissolved solids (TDS) in water samples, causing a transition from rock-dominated areas to the evaporation zone (Krishna Kumar et al. 2014; Satheeskumar et al. 2021). The movement of sampling locations towards the evaporation zone, away from the rock-water interaction zone, demonstrates an elevation in  $\text{Na}^+$  and  $\text{Cl}^-$  ions. Additionally, the increased total dissolved solids (TDS) levels could perhaps be attributed to the intrusion of seawater (Satheeskumar et al. 2021).

#### Base exchange indices

Base exchange indices are typically used in regional hydrogeochemical studies to indicate salinizing or freshening phenomena of aquifers that have been freshened or salinized in the past. Generally, base exchange indices are represented as salinized or freshened facies or into a state of equilibrium (Stuyfzand 2008).

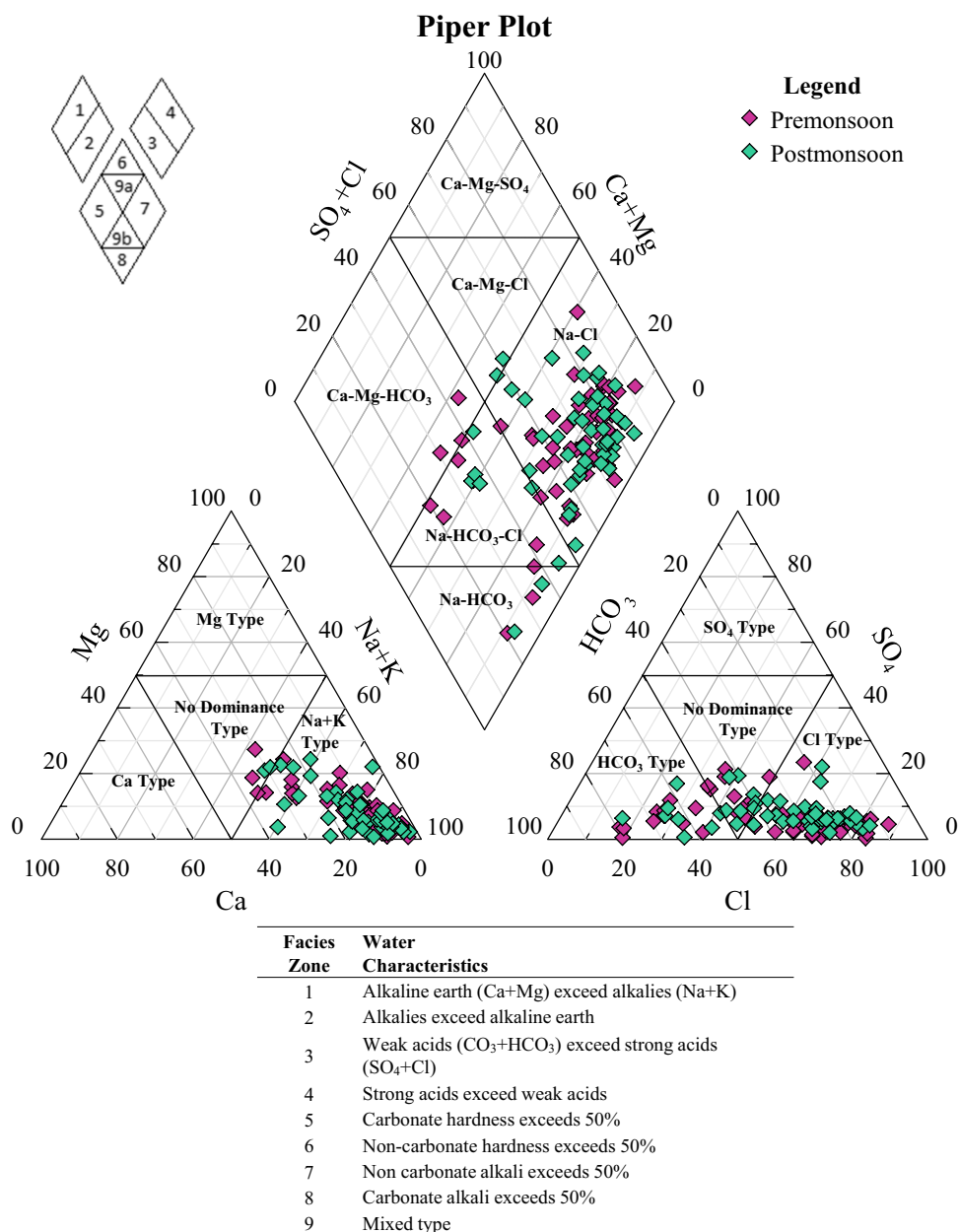
**Schoeller classification (chloroalkaline indices)** Chloroalkaline indices are helpful to understand the evolution of groundwater chemical composition and rock-water interaction (Gowd 2005; Islam et al. 2017). To validate the ion exchange processes that take place in an aquifer medium, Scholler (1965) developed the chloroalkaline indices, and he has provided the following computation of CAI-I and CAI-II

$$\text{CAI - I} = [\text{Cl}^- - (\text{Na}^+ + \text{K}^+)]/\text{Cl}^-$$

$$\text{CAI - II} = [\text{Cl}^- - (\text{Na}^+ + \text{K}^+)]/(\text{SO}_4^{2-} + \text{HCO}_3^- + \text{CO}_3^{2-} + \text{NO}_3^-)$$

The units for measuring ionic concentrations are meq/L.

**Fig. 2** Piper diagram for pre- and post-monsoon groundwater samples



CAI-I ranged from -2.59 to 0.39 with a mean -0.20 in pre-monsoon and -2.95 to 0.36 with a mean -0.16 in post-monsoon, correspondingly. However, CAI-II values varies from -0.98 to 2.74 with a mean 0.05 and -0.94 to 1.31 with a mean -0.12 in pre- and post-monsoon, correspondingly (Table 1). It has been revealed that 63% and 69% of samples show negative ratios, whereas 37% and 31% of samples showed positive ratios for both CAI I and CAI II indices in pre-and post-monsoon, correspondingly (Figs. 4a, b, and 5a, b). The positive value of CAI indicates base exchange reaction whereas negative value for the chloroalkaline disequilibrium. This study demonstrated that the indirect cation exchange process is prevalent during both seasons (Table 1).

**Base exchange index (r1)** The mathematical demonstration of the base exchange index, which is used for groundwater type categorization, is presented as follows:

$$r1 = (Na^+ - Cl^-)/SO_4^{2-}$$

The units for measuring ionic concentrations are meq/L. The value of the base exchange index ranged -86.10 to 29.08 with a mean -0.36 in pre-monsoon and -4.18 to 10.18 with a mean -1.19 in post-monsoon (Table 1). The water samples are categorized into two categories according to the base exchange index: those with a Na<sup>+</sup>-HCO<sub>3</sub><sup>-</sup> water type (r1 > 1) and those with a Na<sup>+</sup>-SO<sub>4</sub><sup>2-</sup> water type (r1 < 1). 43% and 52% of samples have r1 values greater than 1

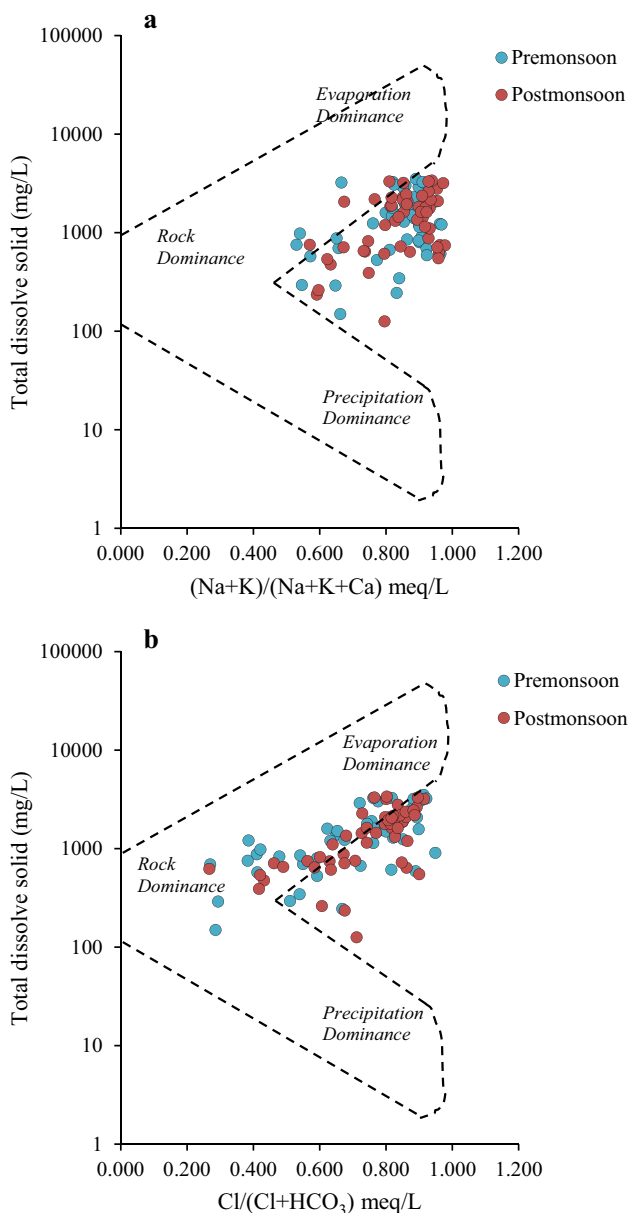


**Fig. 3** **a** Gibbs I diagrams for groundwater samples. **b** Gibbs II diagrams for groundwater samples

( $r_1 >$ ), in pre- and post-monsoon, correspondingly (Fig. 6a, b). Therefore,  $\text{Na}^+\text{-SO}_4^{2-}$  a type of water dominant in pre-monsoon and  $\text{Na}^+\text{-HCO}_3^-$  water type in post-monsoon. The enrichment of  $\text{HCO}_3^-$  may be due to the formation and leaching of bicarbonate produced by the reaction of  $\text{CO}_2$  and rainwater.

**Meteoric genesis index ( $r_2$ )** The meteoric genesis index is another method that can be used to categorize the types

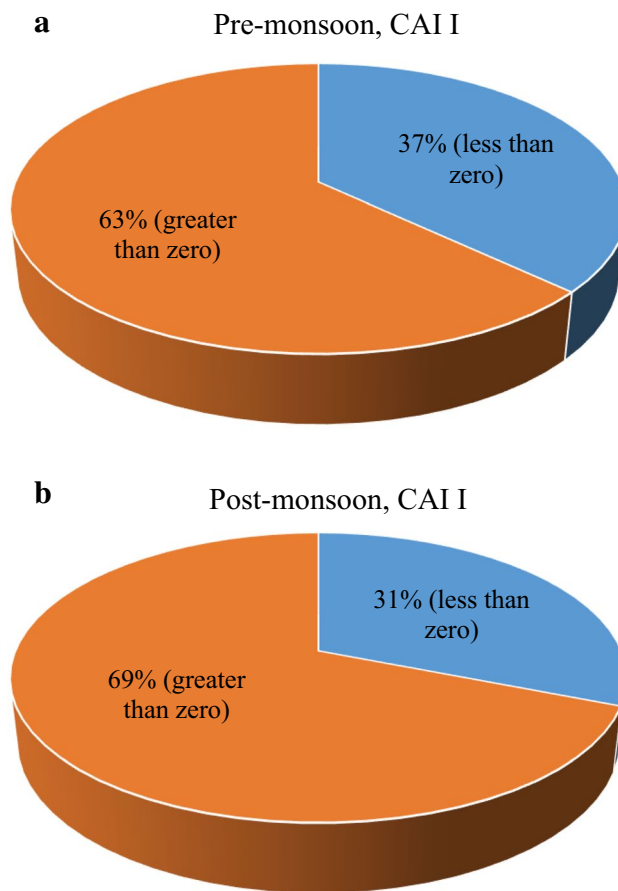


**Fig. 4** **a** Chloroalkaline indices' (CAI I) plots for pre-monsoon samples. **b** Chloroalkaline indices' (CAI I) plots for post-monsoon samples

of groundwater. The following equation is used to give an expression for these meteoric genesis indices:

$$r_2 = \frac{[(\text{K}^+ + \text{Na}^+) - \text{Cl}^-]}{\text{SO}_4^{2-}}$$

The units for measuring ionic concentrations are meq/L. Base exchange index grouped the groundwater as a shallow meteoric water type ( $r_2 > 1$ ) or a deep meteoric water type ( $r_2 < 1$ ) based on its numeric value. It ranged  $-84.91$  to  $29.24$  with a mean  $-0.20$  in pre-monsoon and  $-4.17$  to  $10.22$  with a mean  $1.26$  in post-monsoon (Table 1). then, 44% and 52% of samples with  $r_2$  values higher than one are categorized as shallow meteoric groundwater types, whereas 56% and 48% of samples with an  $r_2$  value less than one were classified as deep meteoric groundwater in pre- and post-monsoon, correspondingly (Fig. 7a, b).

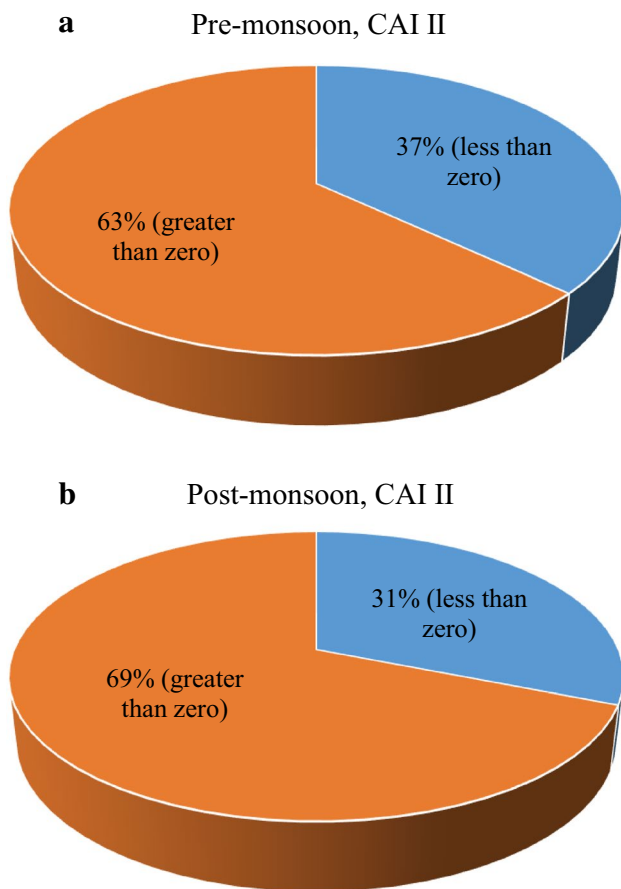


**Fig. 5** **a** Chloroalkaline indices' (CAI II) plots for pre-monsoon samples. **b** Chloroalkaline Indices (CAI II) plots for post-monsoon samples

## Sources of ions

### Natural sources

Saltwater intrusion (SWI) can contribute significantly to the salinity in groundwater. This is mostly owing to the presence of a natural mixing zone and the geographical conditions. Other factors that contribute to salinity include evaporation dominance, rock-water interaction, and precipitation. In addition, human activities that increase non-point sources, such as the return flow from agriculture, the excessive use of fertilizers and pesticides in paddy fields and aquaculture, and the wastewater infiltration, might have an impact on water chemistry.

**Saturation index (SI)** The SI explain the variation of water from equilibrium with regard to the origin of groundwater salinization and the dissolved minerals quantitatively (Jalali 2007, 2010). It is estimated on the basis of the equation that is provided by Lloyd and Heathcote (1985):

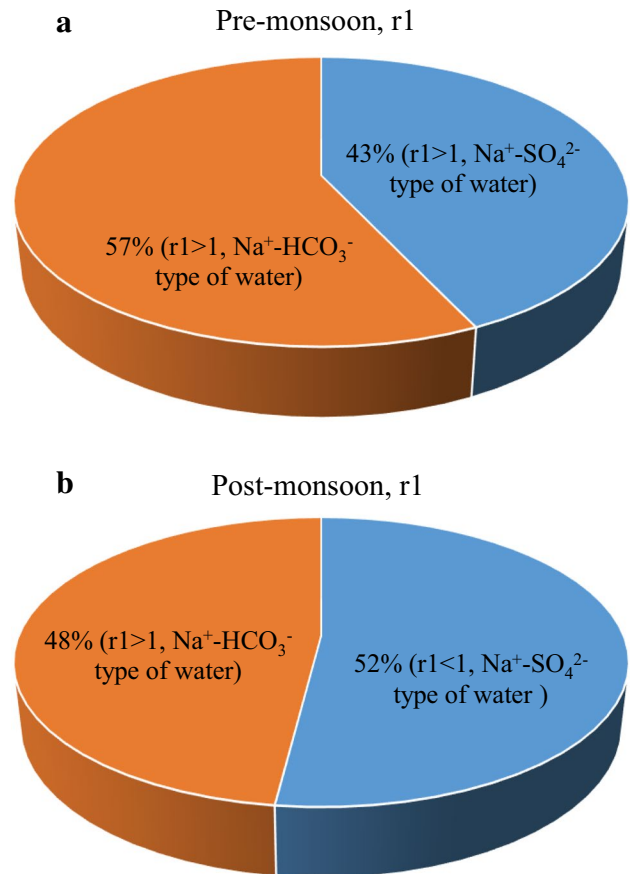


**Fig. 6** **a** Base exchange index ( $r_1$ ) plots for pre-monsoon samples. **b** Base exchange index ( $r_1$ ) plots for post-monsoon samples

$$SI = \log(IAP/K_s)$$

where IAP stands for ion activity product and  $K_s$  is the mineral's solubility product.

The positive SI with iron-bearing minerals reveals the presence of a high concentration of iron in groundwater (Borah et al. 2009; Chakrabarty and Sarma 2011). Graphs of SI of minerals with TDS indicate that 89% and 57% of samples are undersaturated for calcite in pre- and post-monsoon, correspondingly. And, for dolomite, 80% and 52% of samples are undersaturated in pre- and post-monsoon, correspondingly (Fig. 8). The SI value of calcite ranged from  $-2.45$  to  $0.33$  with a mean  $-0.57$  in pre-monsoon and from  $-2.46$  to  $0.40$  with a mean  $-0.29$  in post-monsoon. In contrast, for dolomite, it ranged from  $-4.74$  to  $0.92$  with a mean  $-0.98$  in pre-monsoon and from  $-5.49$  to  $0.75$  with mean  $-0.45$  in post-monsoon.  $\text{Ca}^{2+}$ -bearing minerals (gypsum, anhydrite, fluorite, aragonite, and calcite),  $\text{Mg}^{2+}$ -bearing minerals (dolomite, chrysolite, talc, and sepiolite) are undersaturated ( $SI < 0$ ), while silicate minerals (quartz and chalcedony) and Fe-containing minerals (goethite and hematite) are found

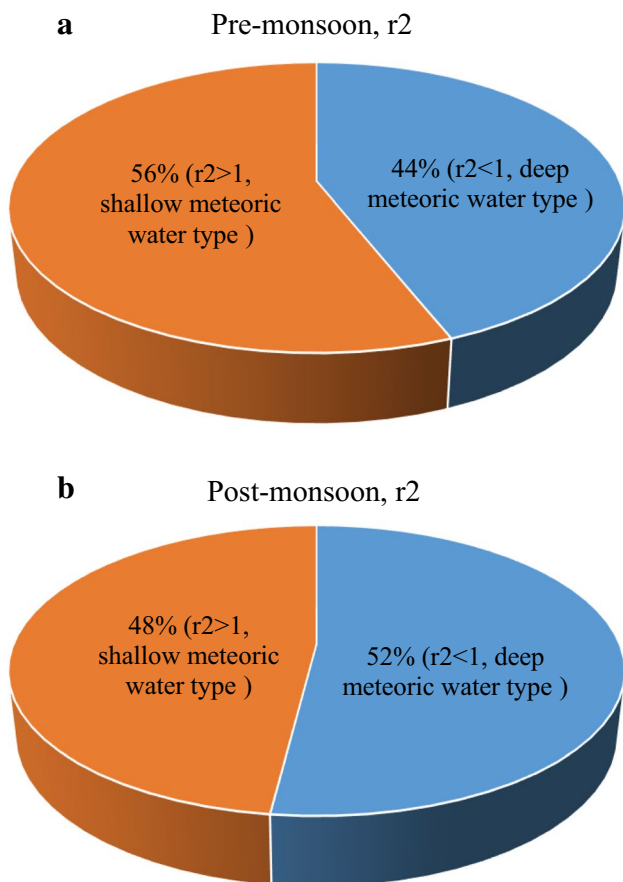
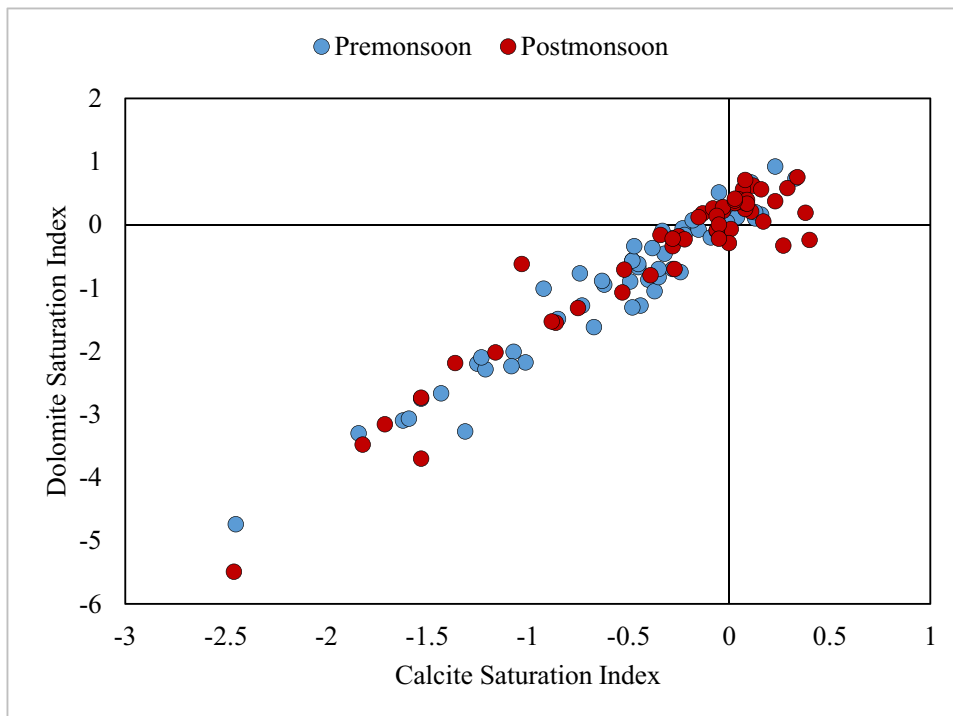


**Fig. 7** a Meteoric genesis index ( $r_2$ ) plots for pre-monsoon samples. b Meteoric genesis index ( $r_2$ ) plots for post-monsoon samples

**Fig. 8** Relation between saturation indices of calcite and dolomite



in saturation state ( $SI > 0$ ) (Fig. 9a, b). The lack of Ca- and Mg-bearing minerals can be inferred from the surrounding lithology, which does not contain rocks rich in Ca and Mg, or if they are present, they are not in a form that can dissolve as Ca and Mg into the water system.

**Saltwater intrusion processes** Ionic ratio comparison, salt-water mixing index, and seawater fraction have been used to acknowledge the potential source of salinity in coastal aquifers.

**1. Ionic ratios**

SWI significantly adds more ions to coastal aquifers (Etikala et al. 2021). High salinity and relatively higher concentrations of  $Na^+$ ,  $Mg^{2+}$ ,  $Br^-$ , and  $Cl^-$  indicate SWI in coastal aquifers. Some good ionic ratios are used to identify SWI processes. Some imperative ionic ratios ( $Na/Cl^-$ ,  $Ca^{2+}/Mg^{2+}$ ,  $K^+/Cl^-$ ,  $Br^-/Cl^-$ , and  $Cl^-/HCO_3^-$ ) have been compared as a potential cause of groundwater salinity. Salinization of groundwater in the coastal zone is predominantly due to SWI and profound deep saline upconing (overexploitation of coastal aquifer) (Vengosh and Rosenthal 1994; Nair et al. 2015; Patel et al. 2016; Sudaryanto and Nailly 2018; Satheeskumar et al. 2021).

- $Na^+/Cl^-$  ratio  
The salinity of water caused by the seawater intrusion is distinguished by a comparatively low  $Na^+/Cl^-$  ratio when compared to both freshwater and seawater (Asare et al. 2021). Saline water has  $Na^+/Cl^-$  ratio



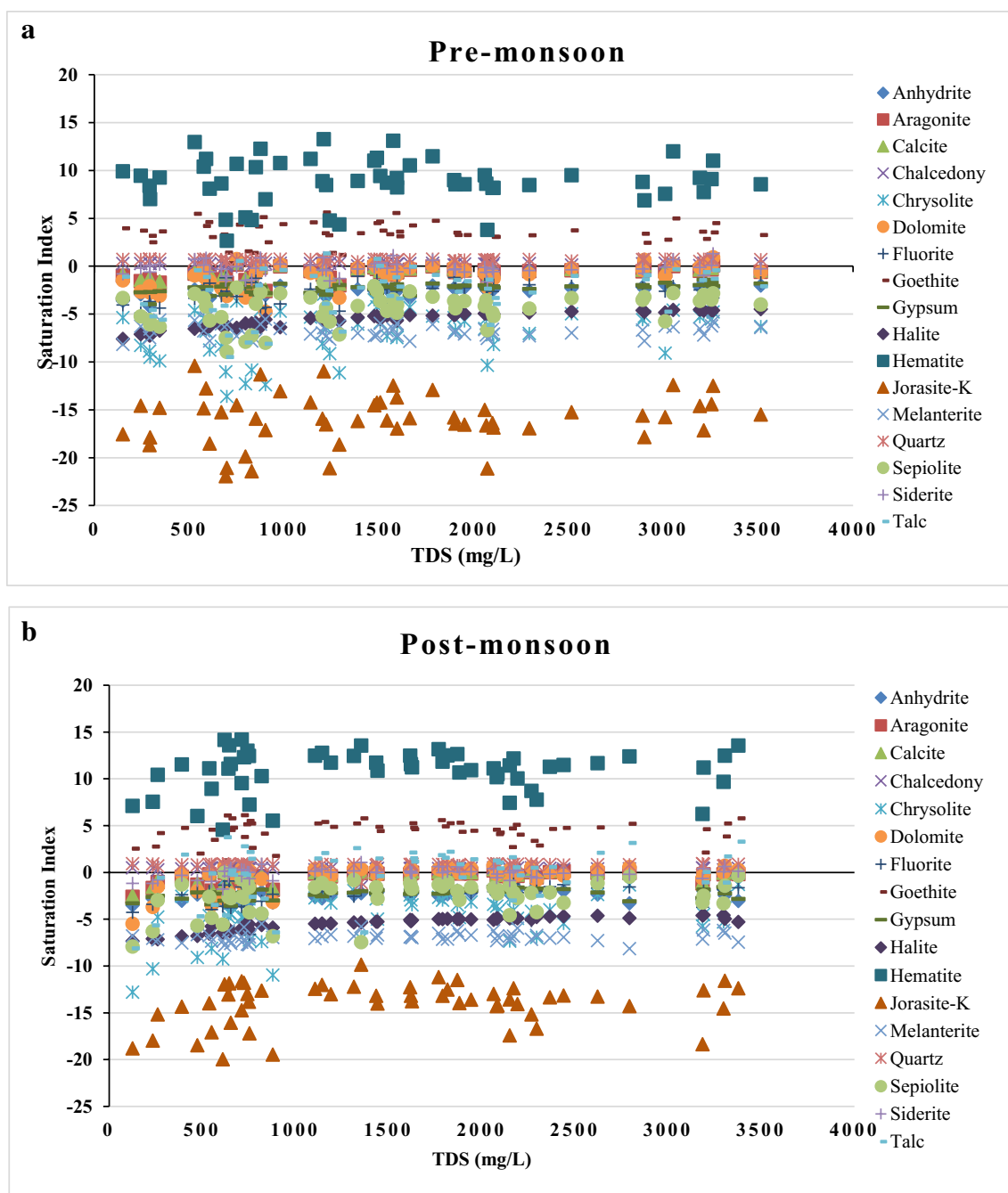


**Fig. 9** **a** Plot of saturation indices and TDS (mg/L) for pre-monsoon. **b** Plot of saturation indices and TDS (mg/L) for pre-monsoon

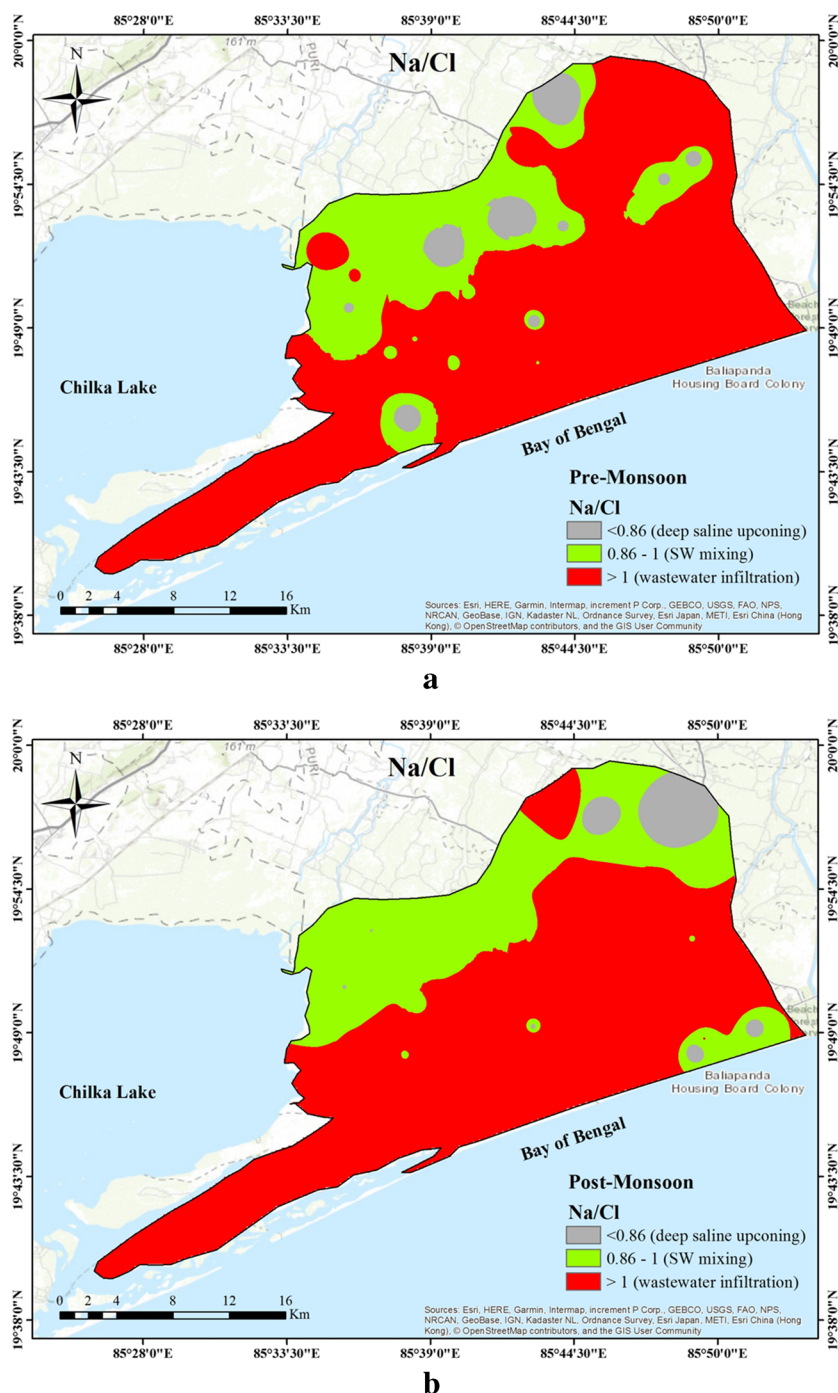
equal to 0.86, freshwater has this value > 1, and the value from 0.86 to 1 indicates the seawater invasion into the freshwater aquifers.  $Na^+/Cl^-$  ratio ranged 0.61 to 3.58 with mean 1.19 and 0.64 to 3.94 with mean 1.16 in pre- and post-monsoon, correspondingly (Table 1 and Fig. 10a, b). In the present study, 37% in pre-monsoon and 33% in post-monsoon samples show  $Na^+/Cl^-$  ratio < 0.86, which indicates SWI into the coastal groundwater (Vengosh and Rosenthal

1994; Nair et al. 2015). On the other hand, 63% of pre-monsoon and 67% of post-monsoon samples show a  $Na^+/Cl^-$  molar ratio > 1, revealing freshwater aquifers in the coastal aquifer.

- $Ca^{2+}/Mg^{2+}$  ratio

A high concentration of  $Mg^{2+}$  compared to  $Ca^{2+}$  with a high TDS value shows saltwater mixing (Kura et al. 2018). If the  $Ca^{2+}/Mg^{2+}$  ratio of < 1 indicates SWI (Moujabber et al. 2006).  $Ca^{2+}/Mg^{2+}$  ratio ranged 0.21

**Fig. 10** **a** Spatial diagram of Na/Cl (pre-monsoon), **b** Spatial diagram of Na/Cl (post-monsoon)



to 6.06 with mean 1.21 and from 0.05 to 14.71 with mean 1.62 in pre- and post-monsoon, correspondingly (Table 1). In the present study, 61% and 63% samples in pre- and post-monsoon, correspondingly showed  $< 1$  value of  $\text{Ca}^{2+}/\text{Mg}^{2+}$  ratio. Thus, the majority of the samples were affected by SWI (Fig. 11a, b).

- $\text{K}^+/\text{Cl}^-$  ratio

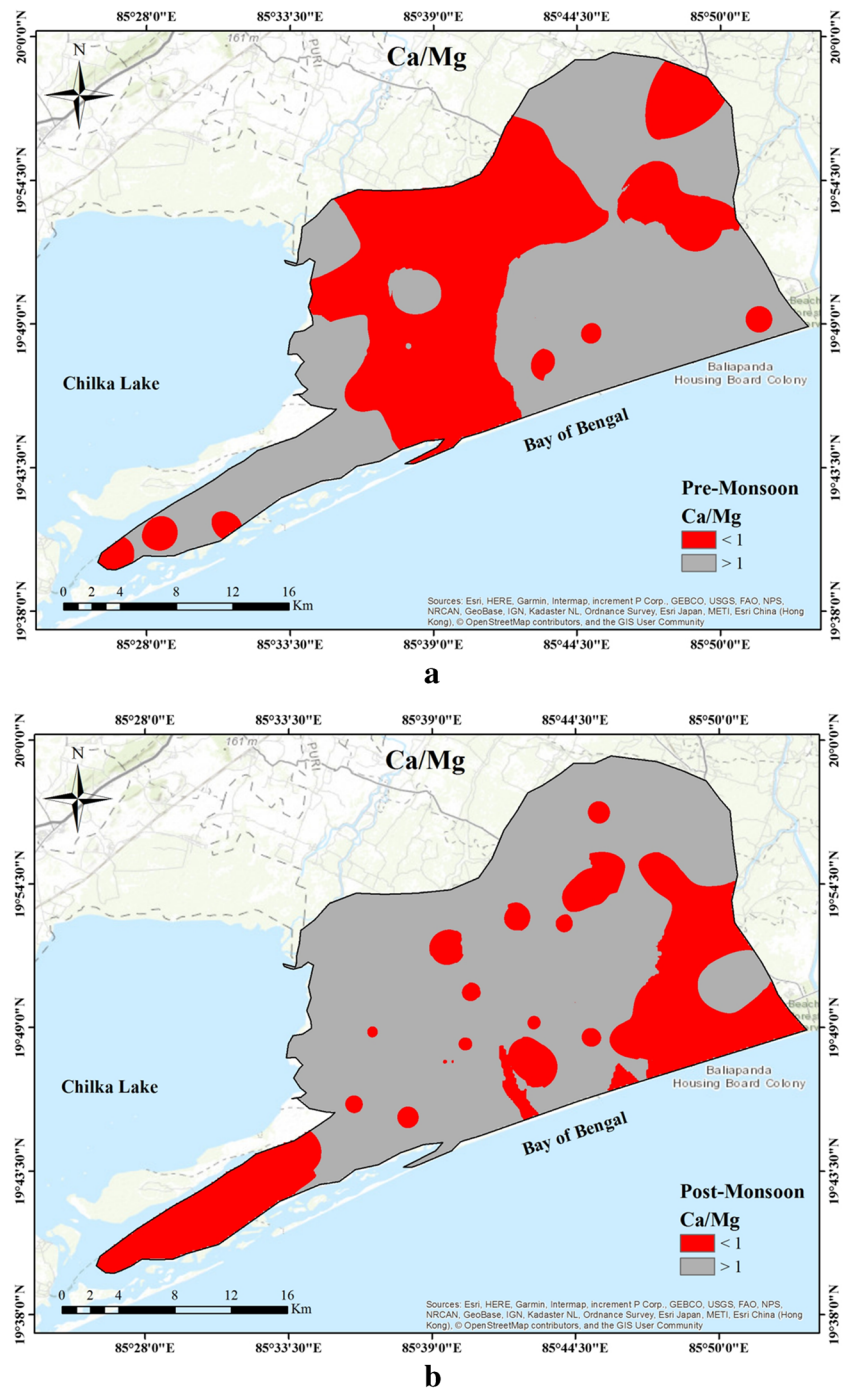
$\text{K}^+/\text{Cl}^-$  ratio below 0.019 show deep saline upconing (Patel et al. 2016).  $\text{K}^+/\text{Cl}^-$  ratio ranged

from 0.001 to 0.058 with a mean value of 0.01 and from 0.001 to 0.063 with a mean value of 0.007 in pre- and post-monsoon, correspondingly (Table 1 and Fig. 12a, b). Then, 81% in pre-monsoon and 90% post-monsoon samples deciphered deep saline upconing.

- $\text{Br}^-/\text{Cl}^-$  ratio

An elevated concentration of halogens, specifically  $\text{Cl}^-$  and  $\text{Br}^-$  in groundwater, indicates SWI.

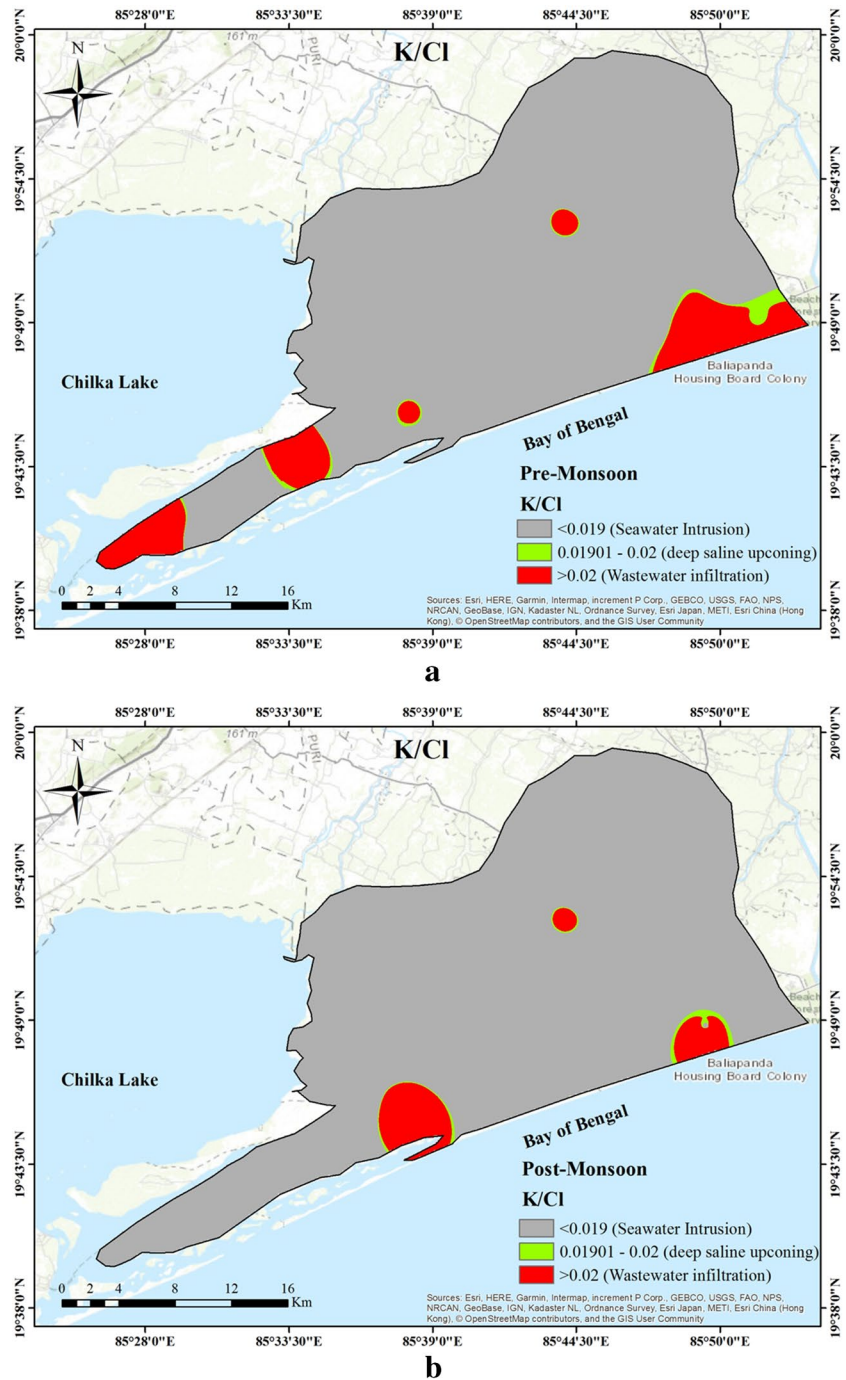
**Fig. 11** **a** Spatial diagram of Ca/Mg (pre-monsoon). **b** Spatial diagram of Ca/Mg (post-monsoon)



The  $\text{Br}^-/\text{Cl}^-$  is considered a reliable tracer of saline water intrusion as both  $\text{Cl}^-$  and  $\text{Br}^-$  are conservative elements, except in the occurrence of a very high amount of organic matter (Vengosh et al. 1999; Kim et al. 2003; Montety et al. 2008; Jia et al. 2017; Gomes et al. 2019; Satheeskumar et al. 2021). The  $\text{Br}^-/\text{Cl}^-$  ratio ranged 0.008 to 0.026 with mean 0.016 and 0.002 to 0.030 with a mean 0.014 in pre- and post-monsoon, correspondingly (Table 1 and

Fig. 13a, b). The  $\text{Br}^-/\text{Cl}^-$  ranged from 0.0033 to 0.0037, with a mean value of 0.0036 in seawater (Kim et al. 2003). The ratio of around 0.02 indicated the agricultural return flow (Montety et al. 2008). Then, 45% and 43% of the samples showed around 0.02 value of  $\text{Br}^-/\text{Cl}^-$  in pre- and post-monsoon, correspondingly. The elevated  $\text{Br}^-/\text{Cl}^-$  ratio deciphered some anthropogenic inputs other than salt-water invasion.

**Fig. 12** **a** Spatial diagram of K/Cl (pre-monsoon). **b** Spatial diagram of K/Cl (post-monsoon)



- $\text{Cl}^-/\text{HCO}_3^-$  ratio

The  $\text{Cl}^-/\text{HCO}_3^-$  ratio is also one of the essential tracers to indicate the saltwater mixing into freshwater aquifers and the origin of salinity. Based on  $\text{Cl}^-/\text{HCO}_3^-$  ratios, there are three categorizations of groundwater that are unaffected (0.5), slightly or moderately (0.6–6.6), and strongly affected (>6.6) affected by the salinization process (Chidambaram et al. 2018; Sudaryanto and Nailly 2018). The ratio ranged from 0.053 to 2.70 with a mean of 0.58 in

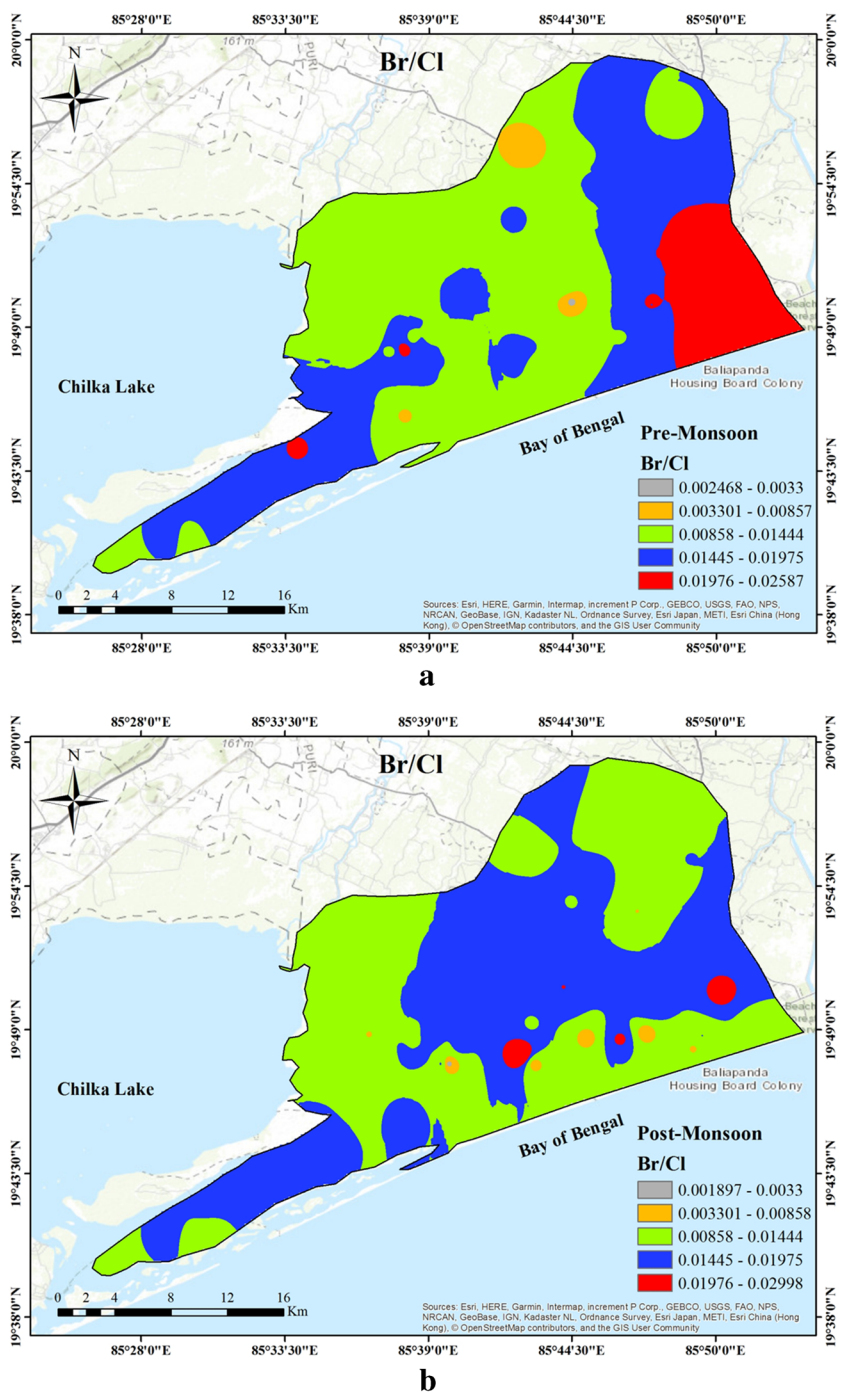
pre-monsoon and from 0.09 to 2.73 with a mean of 0.44 in post-monsoon (Table 1, Fig. 14a and b). Based on the  $\text{Cl}^-/\text{HCO}_3^-$ , 34% and 24% of samples were moderately affected by the salinization process in pre- and post-monsoon, correspondingly.

## 2. Saltwater mixing index (SWMI)

The saltwater mixing index is recognized (Park et al. 2005) to acknowledge the seawater mixing in the coastal aquifer using  $\text{Na}^+$ ,  $\text{Mg}^{2+}$ ,  $\text{Cl}^-$ , and  $\text{SO}_4^{2-}$  as they are



**Fig. 13** **a** Spatial diagram of Br/Cl (pre-monsoon). **b** Spatial diagram of Br/Cl (post-monsoon)



abundant in seawater. The following equation can compute the SWMI:

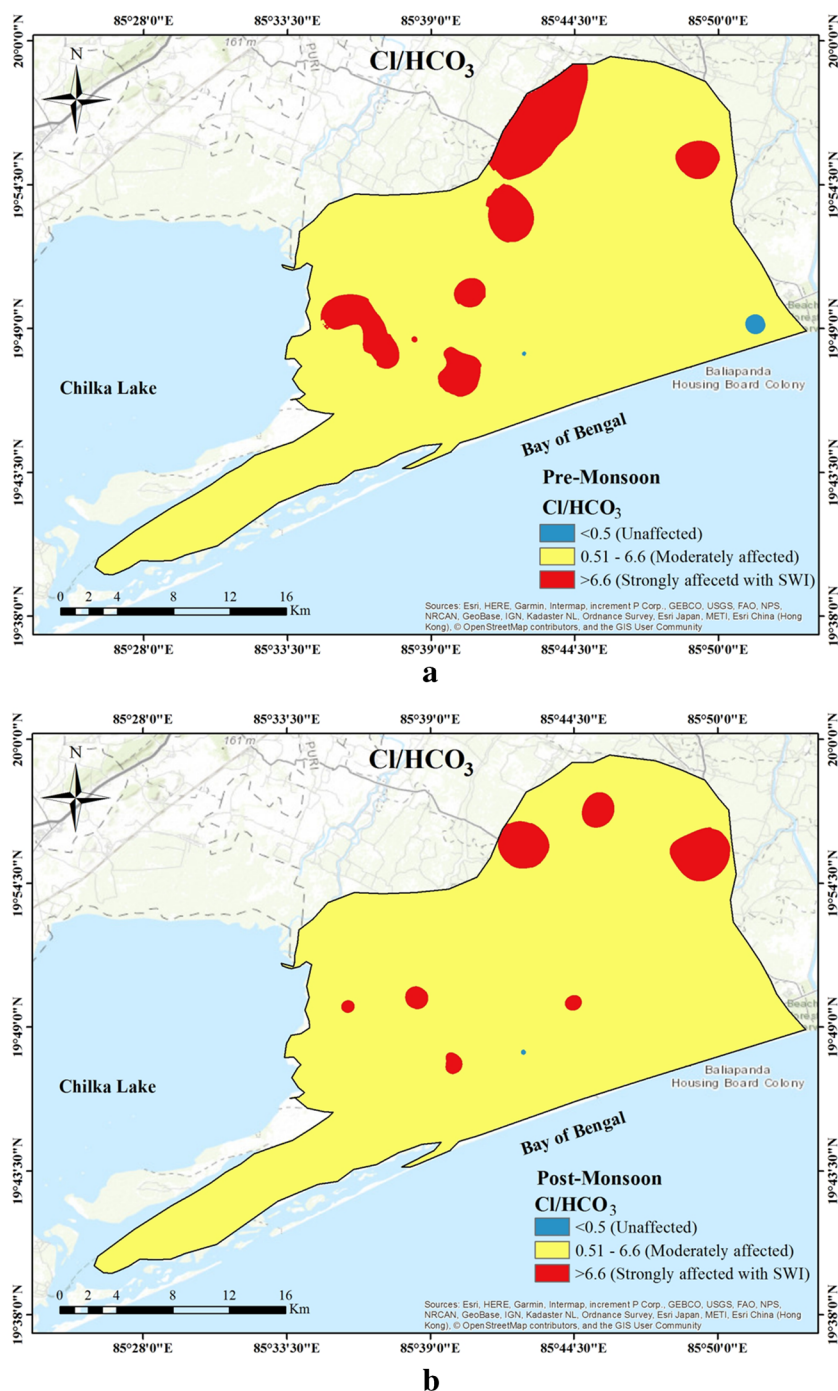
$$SWMI = a \frac{CNa}{TNa} + b \frac{CMg}{TMg} + c \frac{CCl}{TCl} + d \frac{CSO_4}{TSO_4}$$

where constant *a* (0.31), *b* (0.04), *c* (0.57), and *d* (0.08) denote the relative concentration proportion of Na<sup>+</sup>, Mg<sup>2+</sup>, Cl<sup>-</sup>, and SO<sub>4</sub><sup>2-</sup> in seawater (Park et al. 2005). *C<sub>i</sub>*

is the measured value of ions in the groundwater, and *T<sub>i</sub>* is the regional threshold value of respective ions. The threshold values for pre-monsoon were calculated: 89 mg/L for Na<sup>+</sup>, 20.18 mg/L for Mg<sup>2+</sup>, 122 mg/L for Cl<sup>-</sup>, and 18.47 mg/L for SO<sub>4</sub><sup>2-</sup>. For post-monsoon, the threshold value were 102.1 mg/L for Na<sup>+</sup>, 8.75 mg/L for Mg<sup>2+</sup>, 70 mg/L for Cl<sup>-</sup>, and 19.49 mg/L for SO<sub>4</sub><sup>2-</sup>. The threshold value was estimated by the interpreting the cumulative probability curve for both the seasons. If the



**Fig. 14** **a** Spatial diagram of  $Cl/HCO_3$  (pre-monsoon). **b** Spatial diagram of  $Cl/HCO_3$  (post-monsoon)



measured value of SWMI is greater than one, in that case, water may show the effect of seawater interaction with freshwater, whereas this value greater than 3 indicates SWI (Idowu et al. 2017; Idowu and Lasisi 2020; Aladejana et al. 2021).

The current study indicates that 90.74% of samples in pre-monsoon and 94.44% of samples in post-monsoon show the SWMI values greater than unity ( $= 1$ ), indicating the interaction of seawater with freshwater aquifers. Moreo-

ver, 64.81% of samples in pre-monsoon and 72.22% of samples in post-monsoon have shown an SWMI value greater than 3, deciphering the SWI into the freshwater system. SWMI ranged 0.29 to 11.62 in pre-monsoon and 0.53 to 15.66 in post-monsoon (Table 1). The water samples nearby the coast show SWI. In contrast, the samples far from the coast indicate deep saline upconing due to excessive groundwater withdrawal for agriculture and aquaculture. The spatial distribution of SWMI values

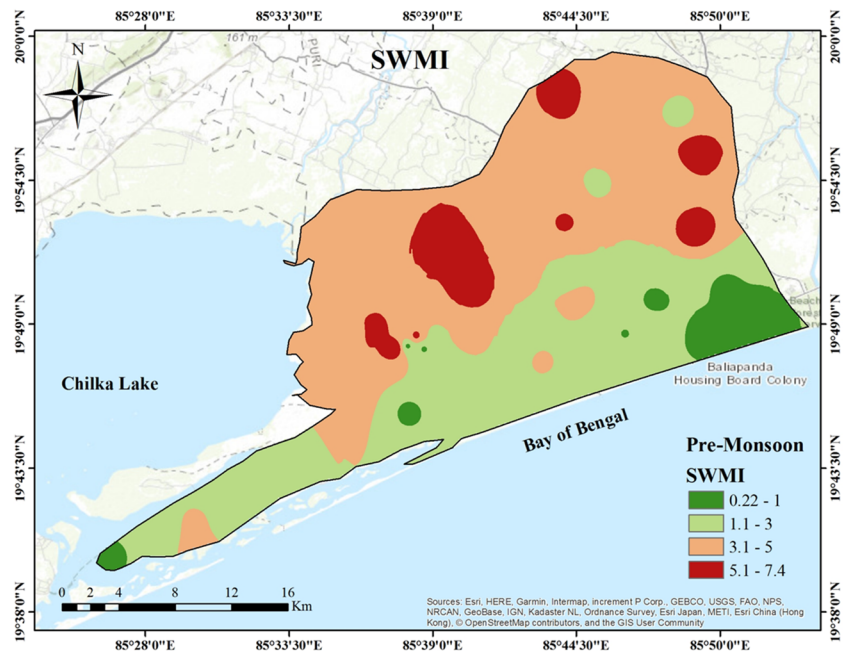
(Fig. 15a, b) shows the seawater mixing in coastal aquifers. There are three categorizations on the map based on SWMI, i.e., (i) freshwater, (ii) fresh-seawater interaction, and (iii) SWI into freshwater aquifer system, laterally through seawater ingression and vertically by deep saline upconing.

3. Seawater percentage (SW%) or seawater fraction (%f sea)

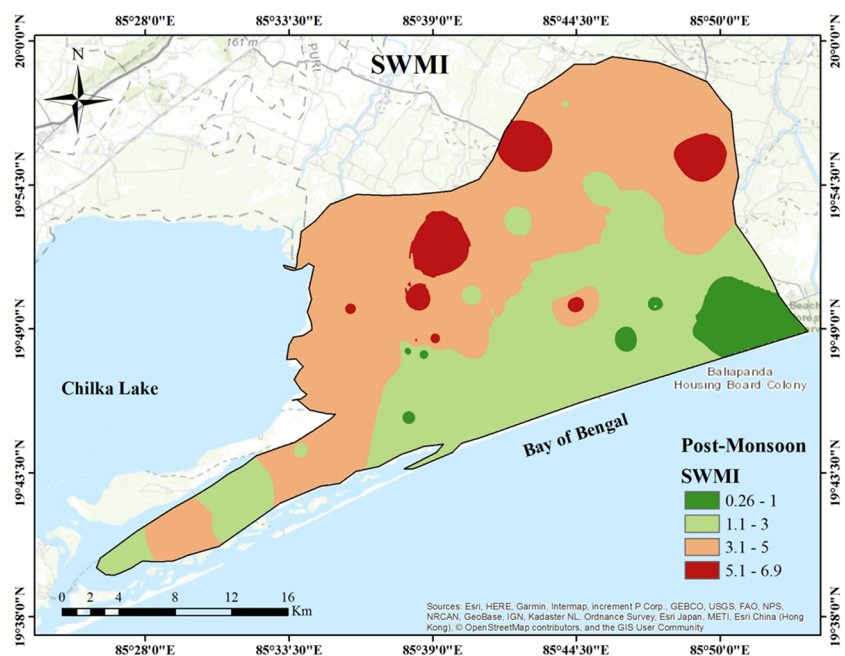
Seawater percentage or seawater fraction is a measurement of seawater percentage in the freshwater aquifers based on the conservative element  $Cl^-$  and it can be estimated by using the following formula:

$$\text{SeawaterFraction}(\%S.W.) = \frac{C_{Cl, sample} - C_{Cl, fresh}}{C_{Cl, sea} - C_{Cl, fresh}} \text{ (Concentration in meq/L)}$$

**Fig. 15** **a** Spatial diagram of SWMI (pre-monsoon). **b** Spatial diagram of SWMI (post-monsoon)



**a**

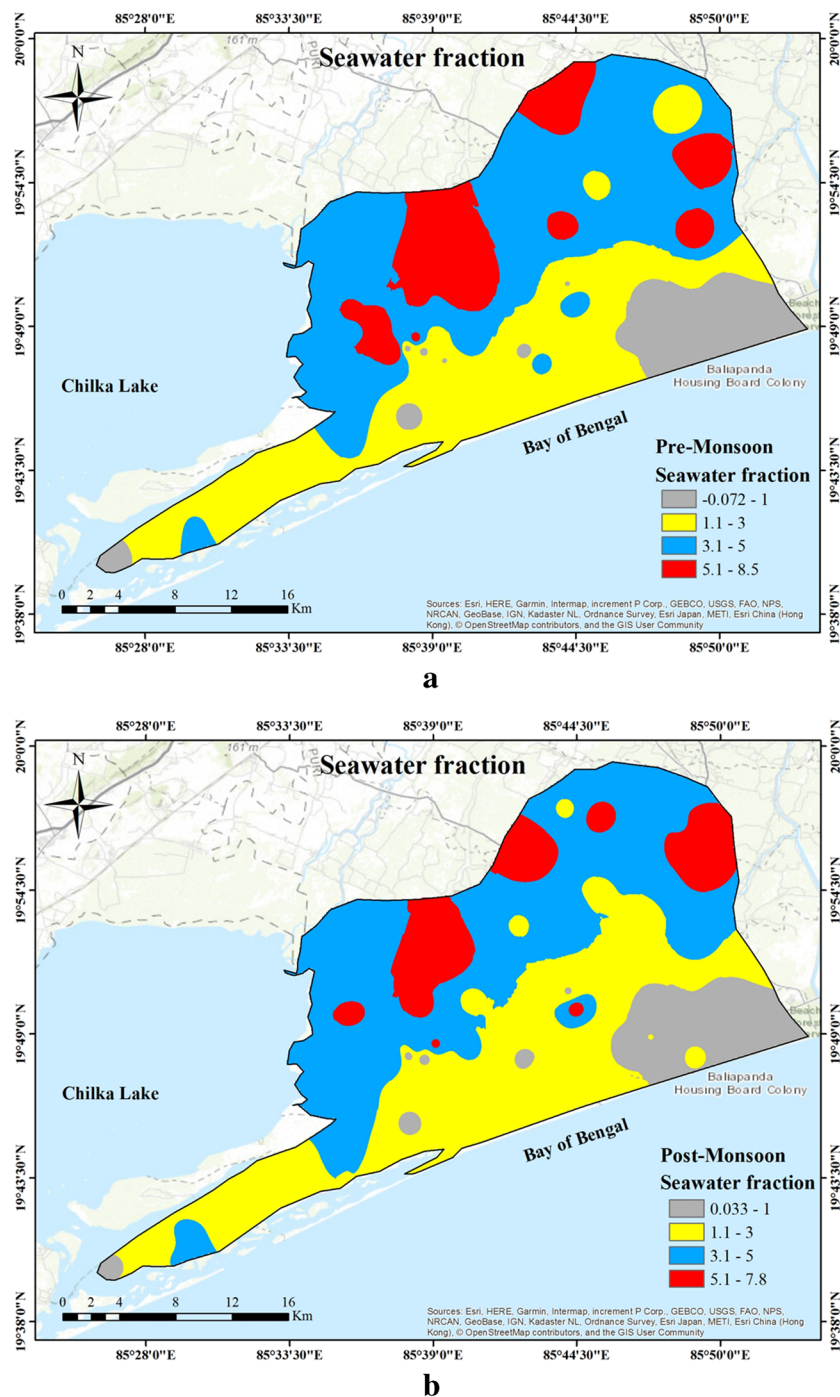


**b**

The seawater fraction can be calculated by assuming that all  $\text{Cl}^-$  should come from seawater and no brine conditions should be available in the area. The water having low  $\text{Na}^+$  and  $\text{Cl}^-$  has been taken as the freshwater samples for the  $\text{Cl}^-$  ions. In this study, the seawater percentage ranged – 0.074 to 8.495 in pre-monsoon and 0.021 to

7.755 in post-monsoon (Table 1, Fig. 16a, b). The sample having a higher value might be contaminated more by SWI. Then, 21% and 17% of samples in pre- and post-monsoon, correspondingly, have  $\text{SW}\% > 5$ . This could be the brine mixing with freshwater aquifers (Mohanty and Rao 2019).

**Fig. 16** **a** Spatial diagram of seawater fraction ( $f\%$ ) (pre-monsoon). **b** Spatial diagram of seawater fraction ( $f\%$ ) (post-monsoon)



### Anthropogenic input of ions

Anthropogenic activities (abundant fertilizers input and its runoff, aquaculture, and wastewater invasion into aquifers from the urbanization and metropolitan cities) also increased the ionic concentration of the groundwater. Relatively high concentrations of  $\text{NO}_3^-$ ,  $\text{Cl}^-$ ,  $\text{Br}^-$ , and  $\text{SO}_4^{2-}$  may result from diverse anthropogenic activities. Anomalous concentrations of  $\text{Cl}^-$  may also be the product of pollution by sewage wastes, excessive use of fertilizers, common salt added to a coconut plantation, fish farming, and leaching of saline residues entrapped within the soil (Raju 2012; Srinivasa-moorthy et al. 2014). The presence of high levels of  $\text{Na}^+$ ,  $\text{Cl}^-$ , and  $\text{SO}_4^{2-}$  in the aquifer may be attributed to the use of  $\text{NaCl}$  and  $\text{Na}_2\text{SO}_4$  salts in fish farming (Barclay et al. 2002). The excess of  $\text{Na}^+$  in groundwater might also come from wastewater infiltration.  $\text{Na}_2\text{SO}_4$  is used instead of  $\text{NaCl}$  for commercial production of aquaculture because it has a corrosive effect on the equipment and reduces the production of microflora in the ponds (Barclay et al. 2002; Jeevanandam et al. 2012). Dissolution of potash feldspar occurs when the molar ratio of  $\text{K}^+/\text{Cl}^-$  exceeds 0.2 values while all values in groundwater are below 0.2, indicating no potash feldspar dissolution (Prasanna et al. 2011).

The concentration of  $\text{Br}^-$  in freshwater ranged from 0.5 to 1 mg/L (WHO 2006). In the present study, all the samples had a  $\text{Br}^-$  concentration are more than 1 mg/L. Fertilizers such as ethyl-dibromide and methyl-bromide may also be the source of  $\text{Br}^-$  concentration other than SWI (Cartwright et al. 2006). The degradation of organic matter could be the reason behind the slight increase of the  $\text{Br}^-$  in most groundwater samples (Montety et al. 2008).

The value of  $\text{NO}_3^-$  in groundwater samples is more than 3 mg/L, indicating human-affected values (Pastén-Zapata

et al. 2014). In the present study, 59.25% of pre-monsoon and all the samples in post-monsoon showed more than 3 mg/L of  $\text{NO}_3^-$  values, which indicates human influence on  $\text{NO}_3^-$  concentration. The high value of  $\text{NO}_3^-$  in post-monsoon may be due to agricultural runoff, poor drainage, and untreated domestic waste. Although the distribution of  $\text{NO}_3^-$  is relatively uniform, some patches of high concentration, near Puri temple area, where degradation of flower waste could be the source of  $\text{NO}_3^-$ . High concentrations of  $\text{NO}_3^-$  in drinking water could be the reason for methemoglobinemia (blue baby syndrome) in newborns and subsequently leads to death by asphyxiation and stomach cancer in adults (Schwendimann et al. 2021).

### Statistical approach

Multivariate statistical techniques, correlation matrix, and principal component analysis (PCA) are efficient means of manipulating, understanding, and symbolizing data concerning groundwater contaminant, quality, and geochemistry (Belkhiri et al. 2011; Emenike et al. 2018; Jampani et al. 2018).

A perfect positive correlation between  $\text{Na}^+$  and  $\text{Cl}^-$  (0.96 in pre- and 0.91 in post-monsoon) could be the indication of halite dissociation (Tables 2 and 3). A good correlation between  $\text{Ca}^{2+}$  and  $\text{SO}_4^{2-}$  (0.59 in post-monsoon) shows gypsum dissolution. Although  $\text{K}^+$  is low in concentration but a good correlation between  $\text{K}^+$  and  $\text{NO}_3^-$  (0.64 in post-monsoon) could be the agricultural runoff as a potential source of  $\text{K}^+$  and  $\text{NO}_3^-$  in the groundwater in post-monsoon.

**Factor analysis** Factor examination is utilized as an arithmetical means to find more significance and define the nature of hydrochemical processes. The study of factor

**Table 2** Correlation matrix for pre-monsoon groundwater samples (N=54)

	pH	EC	Hardness	Ca	Mg	Na	K	$\text{HCO}_3^-$	$\text{Cl}^-$	$\text{F}^-$	$\text{Br}^-$	$\text{SO}_4^{2-}$	$\text{NO}_3^-$
pH	1												
EC	0.103	1											
Hardness	0.083	0.774	1										
Ca	0.097	0.646	0.887	1									
Mg	0.062	0.758	0.941	0.678	1								
Na	0.125	0.956	0.606	0.504	0.592	1							
K	-0.091	0.308	0.352	0.224	0.396	0.182	1						
$\text{HCO}_3^-$	0.269	0.440	0.419	0.266	0.470	0.408	0.457	1					
$\text{Cl}^-$	0.105	0.969	0.764	0.680	0.715	0.948	0.194	0.322	1				
$\text{F}^-$	0.195	-0.069	-0.277	-0.270	-0.246	0.069	-0.245	0.311	-0.084	1			
$\text{Br}^-$	0.134	0.921	0.758	0.662	0.719	0.874	0.201	0.349	0.911	-0.097	1		
$\text{SO}_4^{2-}$	-0.166	0.472	0.436	0.387	0.408	0.448	0.171	0.228	0.375	-0.045	0.514	1	
$\text{NO}_3^-$	-0.180	-0.126	0.022	0.039	0.006	-0.180	0.454	-0.033	-0.219	-0.231	-0.164	0.270	1



scores discloses the degree of influence of each factor on overall water chemistry (Yidana et al. 2018; Emenike et al. 2018; Busico et al. 2018; Madhav et al. 2020). In the current study, four factors are sufficient to explain 79.53% and 81.51% of the variance for the compound matrix in pre- and post-monsoon, correspondingly (Table 4). The total variance of pre-monsoon and post-monsoon is explained by four principal components with its eigenvalue (> 1). The details of the various extracted factors are given below:

Factor 1 explained 44.61% and 42.23% of the total variance in pre- and post-monsoon, correspondingly. Both seasons have high positive loading for EC, hardness, Ca<sup>2+</sup>, Mg<sup>2+</sup>, Na<sup>+</sup>, Cl<sup>-</sup>, Br<sup>-</sup>, and SO<sub>4</sub><sup>2-</sup>. It shows that Na<sup>+</sup>, Ca<sup>2+</sup>, Mg<sup>2+</sup>, Cl<sup>-</sup>, Br<sup>-</sup>, and SO<sub>4</sub><sup>2-</sup> are responsible for high EC. The high value of hardness is directly associated with Ca<sup>2+</sup>, Mg<sup>2+</sup>, Cl<sup>-</sup>, and SO<sub>4</sub><sup>2-</sup>. The positive relation between Na<sup>+</sup> and Cl<sup>-</sup> indicates SWI and, to some extent, halite weathering. The high amount of Br<sup>-</sup> is clearly indicating about SWI in the study area. Ferromagnesian minerals might be the source of the high amount of Mg<sup>2+</sup> in groundwater (Rao 2012). The high value of hardness is directly associated with Ca<sup>2+</sup>, Mg<sup>2+</sup>, Cl<sup>-</sup>, and SO<sub>4</sub><sup>2-</sup>.

Factor 2 explain 12.60% of the total variance and showed high loading for K<sup>+</sup>, HCO<sub>3</sub><sup>-</sup>, and NO<sub>3</sub><sup>-</sup> in pre-monsoon. This factor deciphered intensive agricultural activities. NPK fertilizers used in paddy fields may be the source of K<sup>+</sup> and NO<sub>3</sub><sup>-</sup>. Fish farming might also be accountable for high HCO<sub>3</sub><sup>-</sup> in groundwater (Barclay et al. 2002). The post-monsoon water samples show 16.89% of the total variance and increased loading of pH, HCO<sub>3</sub><sup>-</sup>, and F<sup>-</sup>. It shows the source of ions as biological and natural geogenic sources. In both, the season's high concentration of HCO<sub>3</sub><sup>-</sup> was observed by leaching of HCO<sub>3</sub><sup>-</sup> produced by the reaction of rainwater and CO<sub>2</sub> present in the soil (Raju 2012).

Factor 3 explains 12.40% of the total variance. It was high negative loading of F<sup>-</sup> and high positive loading of SiO<sub>2</sub> in pre-monsoon, showing the lithologic source of silica and fluoride. The high temperature in the pre-monsoon season favors silica weathering in water (Umar and Alam 2012). The post-monsoon water samples show 14.58% of the total variance and increased K<sup>+</sup> and NO<sub>3</sub><sup>-</sup> loading. NPK fertilizers are the source of the high concentration of K<sup>+</sup> and NO<sub>3</sub><sup>-</sup> extensively used in the study area to produce rice.

Factor 4 explains the 9.41% of the total variance and high loading of pH and HCO<sub>3</sub><sup>-</sup> in pre-monsoon. High loading of HCO<sub>3</sub><sup>-</sup> revealed the dissociation of H<sub>2</sub>CO<sub>3</sub> from the soil by the reaction of rainwater and CO<sub>2</sub> (Raju 2012). The post-monsoon water samples show 7.87% of the total variance and high positive loading of SiO<sub>2</sub>. This could be the silicate weathering due to the geogenic factor.

**Table 3** Correlation matrix for post-monsoon groundwater samples (N = 54)

	pH	EC	Hardness	Ca	Mg	Na	K	HCO <sub>3</sub> <sup>-</sup>	Cl <sup>-</sup>	F <sup>-</sup>	Br <sup>-</sup>	SO <sub>4</sub> <sup>2-</sup>	NO <sub>3</sub> <sup>-</sup>
pH	1												
EC	0.094	1											
Hardness	-0.317	0.639	1										
Ca	-0.195	0.514	0.738	1									
Mg	-0.310	0.543	0.895	0.360	1								
Na	0.177	0.899	0.508	0.468	0.394	1							
K	-0.279	0.194	0.336	0.181	0.345	0.103	1						
HCO <sub>3</sub> <sup>-</sup>	0.319	0.481	0.380	0.136	0.436	0.529	0.274	1					
Cl <sup>-</sup>	0.027	0.919	0.690	0.645	0.528	0.953	0.108	0.438	1				
F <sup>-</sup>	0.693	-0.024	-0.383	-0.321	-0.317	0.159	-0.305	0.446	-0.035	1			
Br <sup>-</sup>	0.079	0.915	0.664	0.582	0.534	0.921	0.139	0.443	0.947	-0.053	1		
SO <sub>4</sub> <sup>2-</sup>	-0.050	0.592	0.562	0.591	0.387	0.662	0.175	0.418	0.672	-0.051	0.680	1	
NO <sub>3</sub> <sup>-</sup>	-0.343	-0.216	0.118	-0.019	0.176	-0.302	0.642	-0.163	-0.264	-0.313	-0.255	-0.064	1



**Table 4** Varimax rotated component matrix

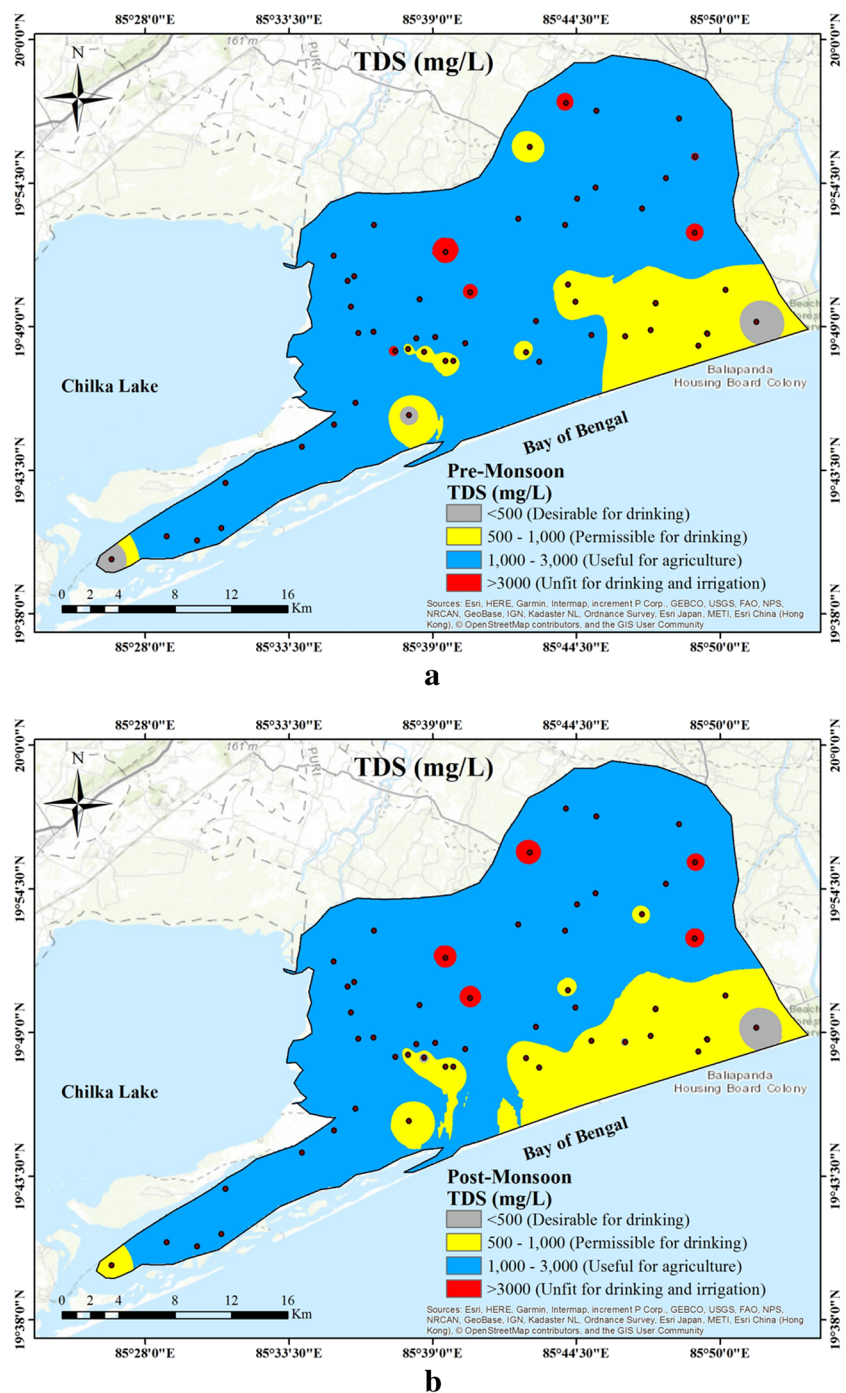
	Component (pre-monsoon)				Component (post-monsoon)			
	1	2	3	4	1	2	3	4
pH	0.077	-0.097	-0.026	0.82	0.019	0.814	-0.246	-0.07
EC	0.965	0.1	-0.118	0.044	0.93	0.121	0.033	0.089
Hardness	0.884	0.193	0.243	0.091	0.766	-0.392	0.352	-0.146
Ca <sup>2+</sup>	0.777	0.081	0.372	0.087	0.685	-0.421	-0.001	-0.113
Mg <sup>2+</sup>	0.836	0.246	0.115	0.083	0.607	-0.263	0.487	-0.127
Na <sup>+</sup>	0.912	0.018	-0.248	0.03	0.921	0.261	-0.068	0.055
K <sup>+</sup>	0.228	0.828	0.129	0.046	0.15	-0.073	0.869	0.152
HCO <sub>3</sub> <sup>-</sup>	0.377	0.546	-0.298	0.538	0.501	0.56	0.38	-0.37
Cl <sup>-</sup>	0.969	-0.059	-0.05	0.04	0.977	0.026	-0.063	0.045
F <sup>-</sup>	-0.146	-0.041	-0.834	0.277	-0.069	0.879	-0.159	-0.158
Br <sup>-</sup>	0.956	-0.036	-0.067	0.016	0.963	0.059	-0.036	0.072
SO <sub>4</sub> <sup>2-</sup>	0.539	0.31	-0.123	-0.419	0.738	-0.069	0.083	-0.278
NO <sub>3</sub> <sup>-</sup>	-0.154	0.729	0.198	-0.356	-0.258	-0.256	0.78	0.138
SiO <sub>2</sub>	-0.101	0.148	0.766	0.134	0.023	-0.228	0.261	0.86
Eigenvalue	6.246	1.765	1.736	1.388	5.912	2.364	2.041	1.094
% total variance	44.614	12.607	12.401	9.412	42.228	16.885	14.577	7.871
% cumulative	44.614	57.221	69.622	79.534	42.228	59.113	73.69	81.507

**Table 5** Ranges of chemical parameters and their comparison with WHO (2006) and BIS (2012) standards of groundwater samples

Parameters (mg/L)	Range (min–max)		Permissible limit		Sample numbers and % of sample exceeding the permissible limit			
	Pre	Post	WHO (2006)	BIS (2012)	WHO (2006)		BIS (2012)	
					Pre-monsoon	Post-monsoon	Pre-monsoon	Post-monsoon
<b>pH</b>	5.76–7.64	6.34–8.14	9.2	8.5	-	-	-	-
<b>Hardness</b>	60–1284	24–1052	500	600	17, 19, 36, 37, 39, 43, 46, 49 (14.8%)	36, 39, 43, 44, 45, 47 (11%)	19, 36, 37, 39, 43, 46, 49 (13%)	36, 39, 44, 45, 47 (9.3%)
<b>TDS</b>	149–3513	125–3377	1500	2000	4, 6, 11–22, 24, 25, 35–40, 44, 45, 46, 49 (48%)	6, 11–21, 25, 26, 32, 34–37, 39, 40, 42–45, 47, 49 (50%)	6, 11–13, 17–19, 21, 25, 35–37, 39, 43, 46, 49 (39.6%)	6, 11, 12, 16, 17, 19, 25, 32, 34–37, 39, 43–45, 47, 49 (33.3%)
<b>Ca<sup>2+</sup></b>	12–288	8–172	200	200	46 (1.8%)	-	46 (1.8%)	-
<b>Mg<sup>2+</sup></b>	2.2–183.34	0.98–243.51	150	100	36 (1.8%)	36 (1.8%)	36, 37, 39, 40 (7.4%)	36 (1.8%)
<b>Na<sup>+</sup></b>	33.4–950.60	21.70– 890.40	200	200	1, 3–7, 11–26, 29, 30, 33–46, 48, 49 (74%)	3–6, 11–26, 29, 30, 32, 34–0, 42–49 (70%)	1, 3–7, 11–26, 29, 30, 33–46, 48, 49 (74%)	3–6, 11–26, 29, 30, 32, 34–40, 42–49 (70%)
<b>K<sup>+</sup></b>	0.50–39.40	0.30–23.90	12	-	22, 26, 39 (5.6%)	39 (1.8%)	-	-
<b>HCO<sub>3</sub><sup>-</sup></b>	40–832	32–612	600	600	36, 39, 44 (5.6%)	36 (1.8%)	36, 39, 44 (5.6%)	36 (1.8%)
<b>SO<sub>4</sub><sup>2-</sup></b>	1.23–182	2.47–126.60	600	400	-	-	-	-
<b>Cl<sup>-</sup></b>	28–1650	16–1510	600	1000	4, 6, 11–21, 25, 35–43, 45, 46, 49 (48%)	6, 11–16, 18–21, 25, 32, 34–36, 39, 40, 42–45, 47, 49 (44.4%)	11, 12, 17, 19, 35–37, 39, 43, 46, 49 (20.4%)	12, 32, 34–36, 43, 45, 47 (14.8%)
<b>F<sup>-</sup></b>	0.02–1.70	0–2.70	1.5	1.2	5 (1.8%)	3, 4, 5 (5.6%)	5 (1.8%)	3, 4, 5 (5.6%)
<b>NO<sub>3</sub><sup>-</sup></b>	BDL–423	3.75–231	50	45	1, 22, 25, 26, 36, 39, 51, 53 (14.8%)	8, 27, 39, 51, 53 (9.3%)	1, 22, 25, 26, 36, 39, 51, 53 (14.8%)	8, 27, 36, 39, 51, 53 (11%)

Concentrations are in mg/L except pH

**Fig. 17** **a** TDS spatial plot for suitability for drinking and agriculture based on Davis and De Wiest (1966) (pre-monsoon). **b** TDS spatial plot for suitability for drinking and agriculture based on Davis and De Wiest (1966) for (post-monsoon)



**Groundwater quality**

**Classification of groundwater for drinking purpose**

To comprehend the groundwater suitability for drinking and community health exercise, hydrogeochemical parameters are compared (Table 5) with the guiding principle prescribed

by WHO (2006) and BIS (2012). According to Davis and De Wiest (1966) categorization, 65% and 63% of samples are inappropriate for drinking purposes in pre- and post-monsoon, correspondingly. The spatial diagram of TDS based on the Davis and De Wiest (1966) is given in Fig. 17a, b. In the context of salinity, 65% and 63% of samples lie in the brackish water category in pre- and post-monsoon, correspondingly (Freeze and Cherry 1979). Based on the Sawyer and Mc. Cartly (1967), 7% and 11% of samples are soft,

**Table 6** Classification of groundwater for agricultural purposes

Quality parameter	Sample range		Range	Classification	Sample (%)	
	(Min–Max)				Pre-monsoon	Post-monsoon
	Pre-monsoon	Post-monsoon				
TDS (Davis and De Wiest, 1966)	149–3513	126–3377	< 500	Desirable for drinking	9	9
			500–1000	Permissible for drinking	26	28
			1000–3000	Useful for agriculture	52	54
			> 3000	Unfit for drinking and irrigation	13	9
Na%	32.92–95.250	39.180–93.839	0–20	Excellent	-	-
			20–40	Good	3.7	3.7
			40–60	Permissible	16.7	13
			60–80	Doubtful	50	41
			> 80	Unsuitable	29	43
			SAR	1.171–34.212	1.271–23.054	0–10
10–18	Good	59	48			
18–26	Fair	2	15			
> 26	Poor	2	-			
RSC (meq/L)	-21.729–8.821	-12.945–5.969	< 1.25	Good	81	81
			1.25–2.5	Medium	6	9
			> 2.5	Bad	13	9
EC ( $\mu\text{S}/\text{cm}$ )	223–7600	125–5500	< 250	Excellent	2	2
			250–750	Good	7	6
			750–2250	Fair	37	38
			> 2250	Poor	54	54
KR	0.469–12.629	0.601–14.886	< 1	Suitable	15	9
			1–2	Marginally suitable	11	22
			> 2	Unsuitable	74	67
MH	14.169–82.979	6.364–95.254	< 50	Suitable for irrigation	39	37
			> 50	Harmful for irrigation	61	63

20% and 11% of samples are slightly hard, 27% and 47% of samples are moderately hard, and 46% and 31% of samples are very hard in pre- and post-monsoon, correspondingly. As per  $\text{Na}^+$  values, 74% and 70% of samples are beyond the permissible limit of WHO (2006) and BIS (2012) in pre- and post-monsoon, correspondingly.

#### Classification of groundwater for irrigation purpose

The significant chemical parameters for determining the degree of the usefulness of groundwater for irrigation are EC, %Na, salinity hazard, SAR, RSC, Kelly's index, and magnesium hazard.

**Electrical conductivity (EC) and percent sodium (%Na)** The EC and  $\text{Na}^+$  are important parameters to classify water quality for agricultural use. The %Na is weighed concerning relative proportions of cations ( $\text{Na}^+$ ,  $\text{K}^+$ ,  $\text{Ca}^{2+}$ , and  $\text{Mg}^{2+}$ ), and a higher %Na negatively impacts soil permeability.

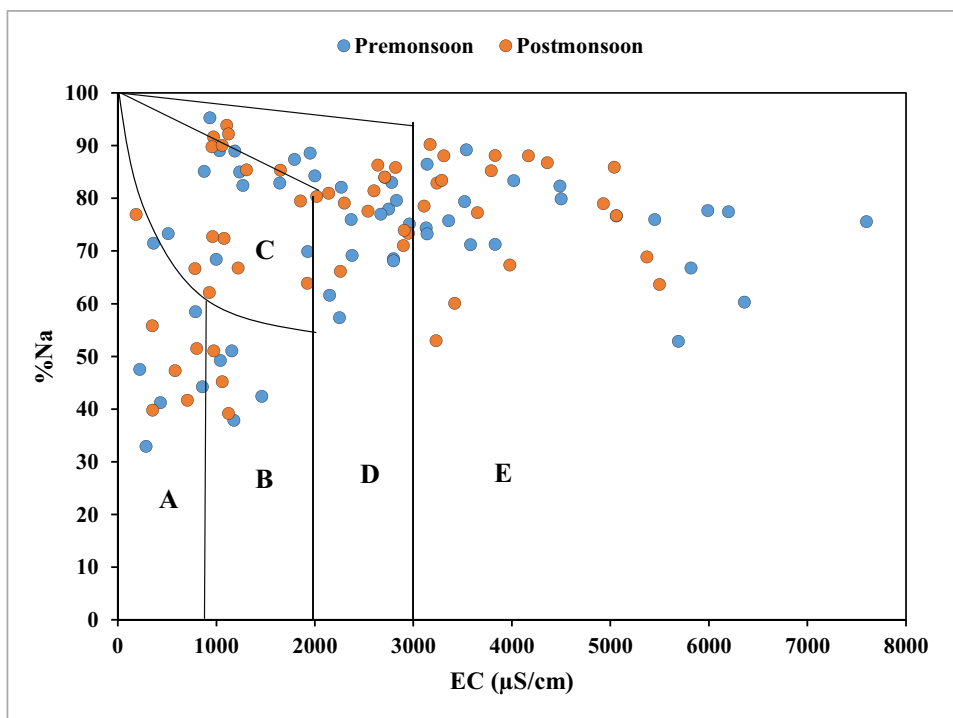
Normally, higher %Na in irrigation water should not exceed 60% (Singh et al. 2015). It is calculated according to the given formula:

$$\% \text{Na} = [(\text{Na}^+ + \text{K}^+)/(\text{Na}^+ + \text{K}^+ + \text{Ca}^{2+} + \text{Mg}^{2+})] * 100$$

The units for measuring ionic concentrations are meq/L.

Based on the %Na classification, 3.7% of samples fall under the good category in both seasons, 16.7% and 13% of samples fall under the permissible category, 50% and 41% of samples fall under the doubtful category, while 29% and 43% of samples fall under unsuitable category in pre- and post-monsoon, correspondingly (Table 6). The water suitability can also be examined by plotting the values of %Na against corresponding values of EC on the Wilcox diagram (Fig. 18). Wilcox diagram (1948) represents that 5.6% and 7.4% of samples lie under excellent to good, 17% and 20% of samples are good to permissible, 11% and 7% of samples lie in permissible to the doubtful range, 33% and 32% of samples lies in doubtful to unsuitable, and 33% and 33% of

**Fig. 18** Groundwater classification based on electrical conductivity and percent sodium (Wilcox diagram 1948) ((A) excellent to good, (B) good to permissible, (C) permissible to doubtful, (D) doubtful to unsuitable, and (E) unsuitable)



samples lies in unsuitable class in pre- and post-monsoon, correspondingly.

**Salinity (EC) hazard** The groundwater has also been classified based on EC (Table 6) and categorized accordingly. As per Richards (1954) classification, 2% of samples fall under the excellent class (C1) in both the seasons, 7% and 6% of the samples lie in good category (C2) in pre- and post-monsoon, correspondingly, while 37% of samples lie in fair class and 54% of samples in poor class in both seasons.

**Sodium adsorption ratio (alkali hazard)** The most frequent method to evaluate sodicity in water and soil is called the SAR. The following equation estimates the SAR

$$SAR = Na^+ / [(Ca^{2+} + Mg^{2+})/2]^{1/2}$$

The units for measuring ionic concentrations are meq/L.

The SAR values ranged from 1.17 to 34.2 meq/L with a mean 10.6 meq/L in pre-monsoon and 1.27 to 23.05 meq/L with a mean 11.45 meq/L in post-monsoon (Table 6). This indicates that in both seasons, all samples came under the S1 category, considered excellent and could be used for irrigational and agricultural activities. According to Richards (1954) categorization on SAR values (Table 5), 37% of samples fall under the excellent category in both seasons, 59% and 48% of samples fall under good quality, 2% and 15% of samples fall in fair class in pre- and post-monsoon,

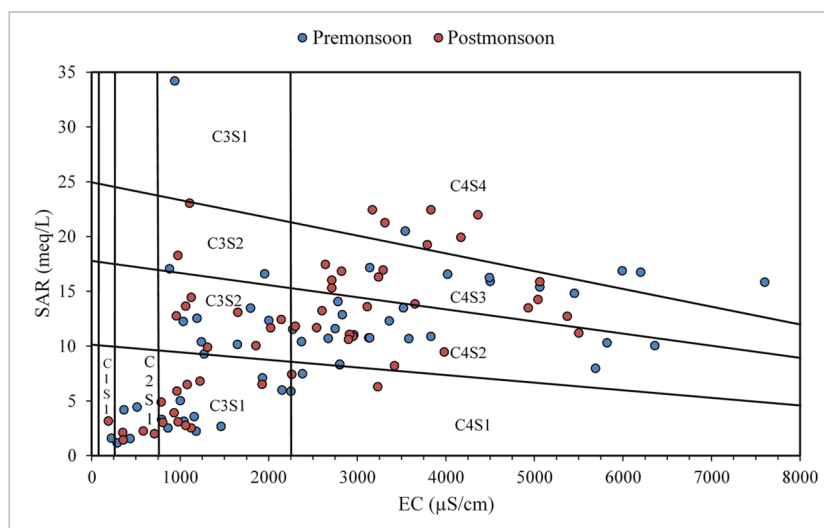
correspondingly, and 2% of samples were poor class in pre-monsoon season.

- U.S. salinity laboratory diagram  
 U.S. salinity diagram (USSL Diagram 1954) has been applied for water classification regarding crop productivity. On the basis of this categorization, 2% of samples fall into the low salinity and low sodium (C1S1) zone in both seasons. 7% of samples fall in medium salty and low sodium (C2S1) in both seasons, which is suitable for all plants. 19% of samples in both seasons fall in high salty and low sodium (C3S1), which need proper drainage for irrigation. 19% of samples in both seasons lies in high saline and medium to very high sodium (C3S2, C3S3, C3S4), which are unsuitable for irrigation. 4% of samples in both seasons fall in very high salty and low sodium (C4S1), which requires a sound drainage system. 31% and 19% of samples fall under the very high salty and medium sodium category (C4S2) in pre- and post-monsoon, correspondingly, which was dangerous for soil. Whereas 19% and 31% of samples fall in very high salty and very high sodium (C4S3 and C4S4), in pre- and post-monsoon which were unsuitable for irrigation (Fig. 19).

**Residual sodium carbonate (RSC)** Sodium adsorption in the soil is amplified to a greater degree when the RSC value is high. RSC has been deliberated to establish the dangerous impact of



**Fig. 19** Groundwater classification on the basis of salinity hazard and alkali hazard (after USSS Diagram 1954)



$\text{CO}_3^{2-}$  and  $\text{HCO}_3^-$  on water excellence for farming use (Eaton 1950). The RSC can be calculated using the following equation:

$$\text{RSC} = (\text{CO}_3^{2-} + \text{HCO}_3^-) - (\text{Ca}^{2+} + \text{Mg}^{2+})$$

The units for measuring ionic concentrations are meq/L.

According to Eaton classification, 81% of samples were categorized within good quality (< 1.25 meq/L) in both seasons, 6% and 9% under medium quality (1.25–2.5 meq/L), and 13% and 9% under bad quality (> 2.5 meq/L) for irrigation purpose in pre- and post-monsoon, correspondingly (Table 6).

**Kelly's index** Kelly's Index is one of the parameters to assess water quality for farming. For computing KI, Kelly (1940) and Paliwal and Singh (1967) have provided the following equation:

$$\text{KI} = [\text{Na}^+]/[\text{Ca}^{2+} + \text{Mg}^{2+}]$$

The units for measuring ionic concentrations are meq/L.

Categorization of water for irrigation based on Kelly's ratio value:

1. KI value < 1—suitable
2. KI value (1–2)—marginally suitable
3. KI value > 2—unsuitable

Based on Kelly's index (KI), groundwater classifies into three classes. KI value is less than one indicates the suitability of water for farming, within 1–2 indicates marginally suitable. KI value > 2 shows the water is not suitable for agriculture. The KI values of groundwater samples ranged from 0.47 to 12.63 with a mean 3.57 and 0.60 to 14.89 with a mean 4.16 in pre- and post-monsoon, correspondingly (Table 6). Based on Kelly's index, 74% and 67% of samples were unsuitable for irrigation in pre- and post-monsoon, correspondingly.

**Magnesium hazard (MH)** The magnesium hazard was introduced by Szabolcs and Darab (1964) as a method for determining the quality of water worth framing. In most cases, the high intensity of  $\text{Mg}^{2+}$  in irrigated soil is caused by the exchangeable  $\text{Na}^+$  in the soils. Sodication in soils is intensified when there is a greater ratio of  $\text{Mg}^{2+}$  to  $\text{Ca}^{2+}$ . It causes the scattering of clay particles. Since  $\text{Mg}^{2+}$  acts similarly to  $\text{Na}^+$ , this causes damage to the structure of the soil and lowers its relative hydraulic conductivity (Raju 2012; Patel et al. 2016). Therefore, water having high  $\text{Mg}^{2+}$  reduces soil productivity.

The following equation calculates magnesium Hazard:

$$\text{MH} = [\text{Mg}^{2+}]/[\text{Ca}^{2+} + \text{Mg}^{2+}] * 100$$

The units for measuring ionic concentrations are meq/L.

A magnesium ratio of more than 50 is regarded as hazardous and unsuitable for irrigation, as the water is considered unsafe and inappropriate for irrigation since it will harm crop production by rising the basic nature of the soil (Raju et al. 2011). The MH values of the sample ranged from 14.17 to 82.98 with a mean 51.35 in pre-monsoon and from 6.36 to 95.25 with mean 50.37 in post-monsoon. According to the MH, 61% and 63% of samples were not appropriate for irrigation in pre- and post-monsoon, correspondingly (Table 6).

## Conclusions

Overexploitation of groundwater in coastal aquifers enhanced the SWI, which makes groundwater unsuitable for intake (drinking purposes), household and farming use. As per the Gibbs plots, all the samples came under rock dominance which is the principal controlling process for groundwater chemistry

in both seasons. Piper diagram reveals  $\text{Na}^+$  and  $\text{Cl}^-$  as dominant ions that were not only from SWI but also from the dissolution of evaporites and local anthropogenic activities (i.e. municipal waste and agricultural activity).  $\text{Na}^+/\text{Cl}^-$ ,  $\text{Ca}^{2+}/\text{Mg}^{2+}$ ,  $\text{K}^+/\text{Cl}^-$ ,  $\text{Br}^-/\text{Cl}^-$ , and  $\text{Cl}^-/\text{HCO}_3^-$  ratios are used to identify SWI. Around 35% of the samples show  $<0.86$  ratios of  $\text{Na}^+/\text{Cl}^-$  in both seasons. An increase of  $\text{Cl}^-$  concentration in  $\text{Br}^-/\text{Cl}^-$  ratio indicates the source of salinization in aquifers is due to the mixing of seawater. According to  $\text{Ca}^{2+}/\text{Mg}^{2+}$  ratio, 61% and 63% of samples were affected by SWI. Moreover, 64.81% and 72.22% of samples in pre- and post-monsoon, correspondingly, were greater than 3, indicating saline water intrusion into the freshwater system. SWI has been observed in all instances, indicating a pervasive occurrence. Factor analysis also verified that natural and anthropogenic activities are accountable for major ion contributions in the groundwater. A total of 65% and 63% of samples are unfit for drinking practice in pre- and post-monsoon, correspondingly. Irrigation water classified based on %Na, 79% and 84% of samples were doubtful to the unsuitable category in pre- and post-monsoon, correspondingly. SWI is a dynamic process, which is why the groundwater must be continuously monitored in the coastal aquifers. This study will help to differentiate the non-contaminated freshwater aquifers from the contaminated aquifers.

## Competing interests

The authors declare no competing interests.

**Acknowledgements** First author is thankful to the Hydrogeology and Environmental Geochemistry Lab, School of Environmental Sciences for providing laboratory facilities for generating the data.

**Author contribution** The conceptualization and methodology of the study were collective efforts of all of the authors. Jyoti Kushawaha has done the investigation and formal analysis, validation, data curation, interpretation, and writing of original draft preparation. Janardhana Raju Nandimandalam has made the investigation, validation, visualization, interpretation, editing, and supervision. Dr. Sugghosh Madhav and Amit Kumar Singh have contributed in statistical analysis, validation, data curation, and editing. The final manuscript has been read and approved by all of the authors.

**Funding** The author Jyoti Kushawaha has availed the funding from the Council for Scientific and Industrial Research (CSIR-NET, File No. 09/263(1148)/2018-EMR-I) during her research related to this publication.

**Data availability** All the data generated during the study are included in this research publication and reviewed by all authors. The data is available from the corresponding author, upon request.

## Declarations

**Ethical approval** Not applicable.

**Consent to publish** The authors have consent to publish this work.

## References

- Aladejana JA, Kalin RM, Sentenac P, Hassan I (2021) Groundwater quality index as a hydrochemical tool for monitoring saltwater intrusion into coastal freshwater aquifer of Eastern Dahomey Basin, Southwestern Nigeria. *Groundw Sustain Dev* 1(13):100568
- APHA (2012) Standard methods for the examination of water and wastewater, 22nd edn. American Public Health Association, American Water Works Association, Water Environment Federation, Washington
- Asare A, Appiah-Adjei EK, Ali B, Owusu-Nimo F (2021) Assessment of seawater intrusion using ionic ratios: the case of coastal communities along the Central Region of Ghana. *Environ Earth Sci* 80:1–4
- Barclay TM, Hicks RG, Lemaire MT, Thompson LK, Xu Z (2002) Synthesis and coordination chemistry of a water-soluble verdazyl radical. structures and magnetic properties of  $\text{M}(\text{H}_2\text{O})_2(\text{vdCO}_2)_2 \cdot 2\text{H}_2\text{O}$  ( $\text{M} = \text{Co}, \text{Ni}$ ;  $\text{vdCO}_2 = 1, 5$ -dimethyl-6-oxo-verdazyl-3-carboxylate). *Chem Comm* (16):1688–1689
- Bear J, Cheng AHD, Sorek S, Ouazar D, Herrera I (Eds.) (1999) Seawater intrusion in coastal aquifers: concepts, methods and practices, vol 14. Springer Science & Business Media
- Belkhir L, Boudoukha A, Mouni L (2011) A multivariate statistical analysis of groundwater chemistry data. *Int J Environ Res* 5(2):537–544
- BIS (2012) Indian standard, drinking water-specification (second revision). IS: 10500, Bureau of Indian Standards, New Delhi
- Borah KK, Bhuyan B, Sarma HP (2009) Heavy metal contamination of groundwater in the tea garden belt of Darrang district, Assam, India. *E-J Chem* 6(S1):S501-7
- Busico G, Cuoco E, Kazakis N, Colombani N, Mastrocicco M, Tedesco D, Voudouris K (2018) Multivariate statistical analysis to characterize/discriminate between anthropogenic and geogenic trace elements occurrence in the Campania Plain, Southern Italy. *Environ Pollut* 1(234):260–269
- Cartwright I, Weaver TR, Fifield LK (2006) Cl/Br ratios and environmental isotopes as indicators of recharge variability and groundwater flow: an example from the southeast Murray Basin, Australia. *Chem Geol* 231(1–2):38–56
- CGWB (2017) National Aquifer Mapping in the district of Puri, Odisha. Interim Unp. Rep. Central Ground Water Board, South Eastern Region, Bhubaneswar, Odisha. Ministry of Water Resources, RD & GR, Government of India
- Chakrabarty S, Sarma HP (2011) Heavy metal contamination of drinking water in Kamrup district, Assam, India. *Environ Monit Assess* 179:479–486
- Chidambaram S, Sarathidasan J, Srinivasamoorthy K, Thivya C, Thilagavathi R, Prasanna M V, Nepolian M (2018) Assessment of hydrogeochemical status of groundwater in a coastal region of Southeast coast of India. *Appl Water Sci* 8:1–14
- Cloutier V, Lefebvre R, Therrien R, Savard MM (2008) Multivariate statistical analysis of geochemical data as indicative of the hydrogeochemical evolution of groundwater in a sedimentary rock aquifer system. *J Hydrol* 353(3–4):294–313
- Davis SN, De Wiest RJM, Ferris JG, Knowles B, Brown RH, Stallman RW (1966) Groundwater in fractured rocks. New York, Hydrogeology 318
- De Montety V, Radakovitch O, Vallet-Coulomb C, Blavoux B, Hermitte D, Valles V (2008) Origin of groundwater salinity and hydrogeochemical processes in a confined coastal aquifer: case of the Rhône delta (Southern France). *Appl Geochem* 23(8):2337–2349
- Eaton FM (1950) Significance of carbonates in irrigation waters. *Soil Sci* 69(2):123–134
- Emenike CP, Tenebe IT, Jarvis P (2018) Fluoride contamination in groundwater sources in Southwestern Nigeria: assessment using

- multivariate statistical approach and human health risk. *Ecotoxicol Environ Saf* 156:391–402
- Essink GH (2001) Improving fresh groundwater supply—problems and solutions. *Ocean Coast Manag* 44(5–6):429–449
- Etikala B, Adimalla N, Madhav S, Somagouni SG, Keshava Kiran Kumar PL (2021) Salinity problems in groundwater and management strategies in arid and semi-arid regions. *Groundw Geochem: Pollut Remediat Methods* 25:42–56
- Famiglietti JS (2014) The global groundwater crisis. *Nat Clim Chang* 4(11):945
- Ferguson G, Gleeson T (2012) Vulnerability of coastal aquifers to groundwater use and climate change. *Nat Clim Chang* 2(5):342–345
- Freeze RA, Cherry JA (1979) *Groundwater*. Prentice-Hall, Englewood Cliffs, 604
- Glynn PD, Plummer LN (2005) Geochemistry and the understanding of ground-water systems. *Hydrogeol J* 13:263–287
- Gomes OV, Marques ED, Kütter VT, Aires JR, Travi Y, Silva-Filho EV (2019) Origin of salinity and hydrogeochemical features of porous aquifers from northeastern Guanabara Bay, Rio de Janeiro, SE-Brazil. *J Hydrol Reg Stud* 22:100601
- Gowd SS (2005) Assessment of groundwater quality for drinking and irrigation purposes: a case study of Peddavanka watershed, Anantapur District, Andhra Pradesh, India. *Environ Geol* 48:702–712
- Huang G, Sun J, Zhang Y, Chen Z, Liu F (2013) Impact of anthropogenic and natural processes on the evolution of groundwater chemistry in a rapidly urbanized coastal area, South China. *Sci Total Environ* 463:209–221
- Idowu TE, Lasisi KH (2020) Seawater intrusion in the coastal aquifers of East and Horn of Africa: a review from a regional perspective. *Sci Afr* 8:e00402
- Idowu TE, Nyadawa M, K’Orowe MO (2017) Hydrogeochemical assessment of a coastal aquifer using statistical and geospatial techniques: case study of Mombasa North Coast, Kenya. *Environ Earth Sci* 76:1–8
- Islam ARMT, Ahmed N, Bodrud-Doza M, Chu R (2017) Characterizing groundwater quality ranks for drinking purposes in Sylhet district, Bangladesh, using entropy method, spatial autocorrelation index, and geostatistics. *Environ Sci Pollut Res* 24:26350–26374
- Jalali M (2007) Salinization of groundwater in arid and semi-arid zones: an example from Tajarak, western Iran. *Environ Geol* 56:1479–1488
- Jalali M (2010) Groundwater geochemistry in the Alisadr, Hamadan, western Iran. *Environ Monit Assess* 166(1–4):359–369
- Jampani M, Huelsmann S, Liedl R, Sonkamble S, Ahmed S, Amerasinghe P (2018) Spatio-temporal distribution and chemical characterization of groundwater quality of a wastewater irrigated system: a case study. *Sci Total Environ* 636:1089–1098
- Jeevanandam M, Nagarajan R, Manikandan M, Senthilkumar M, Srinivasalu S, Prasanna MV (2012) Hydrogeochemistry and microbial contamination of groundwater from lower ponnaiyar basin, cudalore district, Tamil Nadu, India. *Environ Earth Sci* 67:867–887
- Jia Y, Guo H, Xi B, Jiang Y, Zhang Z, Yuan R, Yi W, Xue X (2017) Sources of groundwater salinity and potential impact on arsenic mobility in the western Hetao Basin, Inner Mongolia. *Sci Total Environ* 601:691–702
- Kelly WP (1940) Permissible composition and concentration of irrigated waters. In: *Proceedings of the ASCF* 66, p 607
- Kim Y, Lee KS, Koh DC, Lee DH, Lee SG, Park WB, Koh GW, Woo NC (2003) Hydrogeochemical and isotopic evidence of groundwater salinization in a coastal aquifer: a case study in Jeju volcanic island, Korea. *J Hydrol* 270(3–4):282–294
- Krishna Kumar S, Bharani R, Magesh NS, Godson PS, Chandrasekar N (2014) Hydrogeochemistry and groundwater quality appraisal of part of south Chennai coastal aquifers, Tamil Nadu, India using WQI and fuzzy logic method. *App Water Sci* 4:341–350
- Kumar M, Panday DP, Bhagat C, Herbha N, Agarwal V (2023) Demystifying the decadal shift in the extent of groundwater in the coastal aquifers of Gujarat, India: a case of reduced extent but increased magnitude of seawater intrusion. *Sci Total Environ* 898:165451
- Kumar M, Rahman MM, Ramanathan AL, Naidu R (2016) Arsenic and other elements in drinking water and dietary components from the middle Gangetic plain of Bihar, India: health risk index. *Sci Total Environ* 539:125–134
- Kura NU, Ramli MF, Sulaiman WN, Ibrahim S, Aris AZ (2018) An overview of groundwater chemistry studies in Malaysia. *Environ Sci Pollut Res* 25:7231–7249
- Lloyd JW, Heathcote JAA (1985) Natural inorganic hydrochemistry in relation to ground water
- Madhav S, Ahamad A, Kumar A, Kushawaha J, Singh P, Mishra PK (2018) Geochemical assessment of groundwater quality for its suitability for drinking and irrigation purpose in rural areas of Sant Ravidas Nagar (Bhadohi), Uttar Pradesh. *Geol Ecol Landsc* 2(2):127–136
- Madhav S, Kumar A, Kushawaha J, Ahamad A, Singh P, Dwivedi SB (2020) Geochemical assessment of groundwater quality in Keonjhar City, Odisha, India. *Sustain Water Resour Manag* 6:1–1
- Madhav S, Raju NJ, Ahamad A, Singh AK, Ram P, Gossel W (2021) Hydrogeochemical assessment of groundwater quality and associated potential human health risk in Bhadohi environs, India. *Environ Earth Sci* 80(17):585
- Masood A, Aslam M, Pham QB, Khan W, Masood S (2022) Integrating water quality index, GIS and multivariate statistical techniques towards a better understanding of drinking water quality. *Environ Sci Pollut Res* 1–17
- Mohanty AK, Rao VG (2019) Hydrogeochemical, seawater intrusion and oxygen isotope studies on a coastal region in the Puri District of Odisha, India. *Catena* 172:558–571
- Mohapatra PK, Vijay R, Pujari PR, Sundaray SK, Mohanty BP (2011) Determination of processes affecting groundwater quality in the coastal aquifer beneath Puri City, India: a multivariate statistical approach. *Water Sci Technol* 64(4):809–817
- Mondal NC, Singh VP, Singh S, Singh VS (2011) Hydrochemical characteristic of coastal aquifer from Tuticorin, Tamil Nadu, India. *Environ Monit Assess* 175(1–4):531–550
- Moujabber ME, Samra BB, Darwish T, Atallah T (2006) Comparison of different indicators for groundwater contamination by seawater intrusion on the Lebanese coast. *Water Resour Manag* 20:161–180
- Nair IS, Rajaveni SP, Schneider M, Elango L (2015) Geochemical and isotopic signatures for the identification of seawater intrusion in an alluvial aquifer. *J Earth Syst Sci* 124:1281–1291
- Paliwal KV, Singh S (1967) Effect of gypsum application on the quality of irrigation waters. *Madras Agric J* 59:646–647
- Park SC, Yun ST, Chae GT, Yoo IS, Shin KS, Heo CH, Lee SK (2005) Regional hydrochemical study on salinization of coastal aquifers, western coastal area of South Korea. *J Hydrol* 313(3–4):182–194
- Pastén-Zapata E, Ledesma-Ruiz R, Harter T, Ramírez AI, Mahlknecht J (2014) Assessment of sources and fate of nitrate in shallow groundwater of an agricultural area by using a multi-tracer approach. *Sci Total Environ* 470:855–864
- Patel P, Raju NJ, Reddy BS, Suresh U, Gossel W, Wycisk P (2016) Geochemical processes and multivariate statistical analysis for the assessment of groundwater quality in the Swarnamukhi River basin, Andhra Pradesh, India. *Environ Earth Sci* 75:1–24
- Piper AM (1944) A graphic procedure in the geochemical interpretation of water-analyses. *EOS Trans Am Geophys Union* 25(6):914–928
- De Pippo T, Donadio C, Guida M, Petrosino C (2006) The case of Sarno River (Southern Italy). Effects of geomorphology on the environmental impacts (8 pp). *Environ Sci Pollut Res* 13:184–191
- Prasanna MV, Chidambaram S, Gireesh TV, Jabir Ali TV (2011) A study on hydrochemical characteristics of surface and sub-surface

- water in and around Perumal Lake, Cuddalore district, Tamil Nadu, South India. *Environ Earth Sci* 63:31–47
- Prusty P, Farooq SH, Zimik HV, Barik SS (2018) Assessment of the factors controlling groundwater quality in a coastal aquifer adjacent to the Bay of Bengal, India. *Environ Earth Sci* 77:1–15
- Purnama S, Marfai MA (2012) Saline water intrusion toward groundwater: issues and its control. *J Nat Resour Dev* 2:25–32
- Radhakrishna I (2001) Saline fresh water interface structure in Mahanadi delta region, Orissa, India. *Environ Geol* 40(3):369–380
- Raju NJ (2012) Arsenic Exposure through groundwater in the Middle Ganga Plain in the Varanasi Environs, India: a future threat. *J Geol Soc* 79:302–314
- Raju NJ, Ram P, Dey S (2009) Groundwater quality in the lower Varuna river basin, Varanasi district, Uttar Pradesh. *J Geol Soc* 73:178–192
- Raju NJ, Shukla UK, Ram P (2011) Hydrogeochemistry for the assessment of groundwater quality in Varanasi: a fast-urbanizing center in Uttar Pradesh, India. *Environ Monit Assess* 173:279–300
- Raju NJ, Ram P, Gossel W (2014) Evaluation of groundwater vulnerability in the lower Varuna catchment area, Uttar Pradesh, India using AVI concept. *J Geol Soc* 83:273–278
- Rao NS (2012) Chemical characteristics of groundwater and assessment of groundwater quality in Varaha River Basin Vishakhapatnam District, Andhra Pradesh India. *Environ Monit Assess* 184:5189–5214
- Richards LA (1954) Diagnosis and improvement of saline and alkali soils. US Department of Agri. Hand book, no 60
- Sahagian D (2000) Global physical effects of anthropogenic hydrological alterations: sea level and water redistribution. *Glob Planet Chang* 25(1–2):39–48
- Sahoo S (2014) Assessment of groundwater recharge using water-table fluctuation method and water-balance model. *Environ Sci Technol* 1:27
- Sahu JK, Das PP, Sahoo HK, Mohapatra PP, Sahoo S (2018) Geospatial analysis and hydrogeochemical investigation of a part of southern Mahanadi delta, Odisha, India. *Himal Geol* 39(1):92–100
- Satheeskumar V, Subramani T, Lakshumanan C, Roy PD, Karunanidhi D (2021) Groundwater chemistry and demarcation of seawater intrusion zones in the Thamirabarani delta of south India based on geochemical signatures. *Environ Geochem Health* 43:757–770
- Sawyer CN, McCarty PL (1967) Chemistry for sanitary engineers. McGraw-Hill, New York
- Schoeller H (1965) Qualitative evaluation of groundwater resources. Methods and techniques of groundwater investigations and development. UNESCO, Paris, pp 54–83
- Schwendimann L, Sivaprakasam I, Buvaneshwari S, Gurumurthy GP, Mishra S, Ruiz L, Sekhar M, Fleiss B, Riotte J, Mani S, Gressens P (2021) Agricultural groundwater with high nitrates and dissolved salts given to pregnant mice alters brain development in the offspring. *Ecotoxicol Environ Saf* 224:112635
- Selvakumar S, Chandrasekar N (2021) Impacts of beach placer mineral mining in the shallow coastal aquifers of Southern Tamil Nadu Coast, India. *Water Sci Sustain* 183–200
- Singh S, Raju NJ, Ramakrishna C (2015) Evaluation of groundwater quality and its suitability for domestic and irrigation use in parts of the Chandauli-Varanasi region, Uttar Pradesh, India. *J Water Resource Prot* 7(07):572
- Srinivasamoorthy K, Gopinath M, Chidambaram S, Vasanthavignar M, Sarma VS (2014) Hydrochemical characterization and quality appraisal of groundwater from Pungar sub basin, Tamilnadu, India. *J King Saud Univ-Sci* 26(1):37–52
- Stuyfzand PJ (2008) Base exchange indices as indicators of salinization or freshening of (coastal) aquifers. In: 20th Salt Water Intrusion Meeting, Naples, Florida, USA. IFAS Research Gainesville
- Sudaryanto, Naili W (2018) Ratio of major ions in groundwater to determine saltwater intrusion in coastal areas. *IOP Conf Ser: Environ Earth Sci* 118:012021
- Suguna S, Sherene T (2019) Assessment of sea water intrusion in ground water samples of selected blocks of Cuddalore District, Tamil Nadu, India. *Madras Agric J* 106:7–9
- Szabolcs I, Darab K (1964) Radioactive technique for examining the improving effect of CaCO<sub>3</sub> on alkali (szik) soils
- Umar R, Alam F (2012) Assessment of hydrogeochemical characteristics of groundwater in parts of Hindon-Yamuna interfluvial region, Baghpat District, Western Uttar Pradesh. *Environ Monit Assess* 184:2321–2336
- USSL (1954) Diagnosis and improvement of saline and alkali soils. USDA Hand Book, 60: 147
- Vengosh A, Rosenthal E (1994) Saline groundwater in Israel: its bearing on the water crisis in the country. *J Hydrol* 156(1–4):389–430
- Vengosh A, Spivack AJ, Artzi Y, Ayalon A (1999) Geochemical and boron, strontium, and oxygen isotopic constraints on the origin of the salinity in groundwater from the Mediterranean coast of Israel. *Water Resour Res* 35(6):1877–1894
- Vijay R, Khobragade P, Mohapatra PK (2011) Assessment of groundwater quality in Puri City, India: an impact of anthropogenic activities. *Environ Monit and Assess* 177:409–418
- World Health Organisation (WHO) (2006) Guidelines for drinking water quality; Geneva, World Health Organisation
- Wilcox LV (1948) The quality of water for irrigation use
- Yidana SM, Bawoyobie P, Sakyi P, Fynn OF (2018) Evolutionary analysis of groundwater flow: application of multivariate statistical analysis to hydrochemical data in the Densu Basin, Ghana. *J Afr Earth Sci* 138:167–176

**Publisher's Note** Springer Nature remains neutral with regard to jurisdictional claims in published maps and institutional affiliations.

Springer Nature or its licensor (e.g. a society or other partner) holds exclusive rights to this article under a publishing agreement with the author(s) or other rightsholder(s); author self-archiving of the accepted manuscript version of this article is solely governed by the terms of such publishing agreement and applicable law.